FINITE ELEMENT ANALYSIS SIMULATING INDENTATION TESTING OF HUMAN VAGINAL TISSUE

By

[2015]

Jennifer M. Melendez

Submitted to the graduate degree program in Bioengineering and the Graduate Faculty of the University of Kansas in partial fulfillment of the requirements for the degree of Master of Science.

_____

Chairperson Sarah Kieweg

_____

Anil Misra

_____

Sarah Wilson

Date Defended: May 14, 2015

The Thesis Committee for Jennifer M. Melendez

certifies that this is the approved version of the following thesis:

FINITE ELEMENT ANALYSIS SIMULATING INDETATION TESTING OF HUMAN VAGINAL TISSUE

_____

Chairperson Sarah Kieweg

Date approved:

Acknowledgments

I would like to thank Dr. Sarah Kieweg for giving me the opportunity to work in the Biofluid Dynamics Laboratory. I am grateful for the support and guidance she has given me throughout my time at KU which has allowed me to extended knowledge in biofluids, tissue mechanics, and finite element analysis. I have also been able to hone my skills in research investigation which I will carry forward into a career in bioengineering.

I am also thankful for the help of my committee members Dr. Sara Wilson and Dr. Anil Misra. Their knowledge of tissue mechanics and finite element proved invaluable to my learning and also in guiding the direction of my research. I would like to extend a thank you to all the professors in the bioengineering, chemical engineering, and biology departments who helped in my learning process.

I would like to recognize my lab group for providing support and feedback during lab meetings. I would also like to extend a special thanks to Mark Pacey for his support and for sharing his knowledge in conjunction with his device design.

Finally, I would like to thank my family for their continued support in my career endeavors. My parents Frank and Bertha continued encouragement has allowed me to succeed both academically and in my career. My brothers Frank and Phillip inspire me to follow my dreams which led me into bioengineering.

Abstract

Finite element analysis has often been used in conjunction with experimental testing to provide in-depth understanding of material properties. The aim of this study was to develop a finite element model to be utilized for the interpretation of indentation testing on human, *in vivo* vaginal tissue. Two distinct models were explored to understand the mechanical material properties and the dynamic influences.

First, a single layer, flat tissue model was evaluated. Small indentation simulation was performed to validate the model according to Hertz theory of elasticity. Once validated for multiple elastic moduli, large deformation was applied. Stress and strain along with force were investigated in relation to the displacement of the indenter into the tissue and the Young's modulus.

Next, the findings of the single layer simulation were compared against preliminary, experimental, indentation, test results. Force-displacement results were assessed. Although fundamental differences including geometric and process variances lead to non-congruent results, highly valuable information was attained including understanding of extreme limits that may be found during *in vivo* experimentation.

Finally, a second model was developed based on the findings of the first single-layer model. This new model incorporated multiple tissue layers for the investigation of influence of adjacent tissue properties on vaginal tissue properties during compression testing.

Interpretations of each model were then discussed and conclusions drawn regarding how changes in the properties provide further understanding of tissue dynamics. Further discussion was also provided on possible changes to enhance the model.

Contents

Table of Figures

1. Background

1.1. Scope

Several studies have utilized finite element modeling to simulate the dynamics of tissue. The main focus of this study was to develop a finite element model to help evaluate and characterize the mechanical properties of phantom tissue mimicking human vaginal tissue. This study extends the evaluation of the phantom material from the direct data collected by the Elevated-surface Vaginal Elastomer (EVE) device and incorporates the data to obtain additional properties as well as understand influences of adjacent tissue found anatomically. It was hypothesized that the model will provide a more thorough understanding of the material mechanics than that from interpretation of experimental data alone.

Using the commercial finite element analysis (FEA) software Abaqus 6.13.3, indentation testing of the tissue was modelled to obtain elasticity characterization of the tissue material. The results were then compared to preliminary EVE experimental data. In addition, the FEA allowed for further characterization such as stress distribution and interaction between the test device and material. The long term goal of this investigation is to develop a model to interpret the vaginal tissue response during *in vivo*, indentation testing.

1.2. Motivation

The motivation for this study is based on the need to develop a drug delivery mechanism for an HIV microbicide. As of 2013, 1.2 million people in the U.S. and 35 million people worldwide were living with HIV/AIDS[1]. As this epidemic continues, many researchers are working to prevent the spread of HIV. Microbicides are currently being developed and tested for this purpose. These microbicides are designed to coat the surface of the vaginal canal or rectum with antiretroviral drugs using gels as the delivery systems. One microbicide has been shown to

reduce the risk of infection by 39 percent [2]. As with any coating process, it is necessary for the fluid to completely coat the surface to maximize the effectiveness. Equally as important is the retention abilities of the gel within the cavity. While the microbicide has been shown to have higher success, resistance by clinical trial participants to adhere to the necessary process has been found in other trials [3]. In order to increase user acceptability, the gel must be able to remain in the cavity without leakage. The relationship between the material properties of the surface and the dynamics of the fluid plays a critical role in how completely the microbicide coats the surface and stays in place. In order to maximize the efficacy and acceptability of these microbicides, understanding of the tissue properties is needed.

This lab group has developed the EVE device for the purpose of performing indentation testing on hydrogel phantoms as well as healthy, *in vivo*, human vaginal tissue. This device will obtain the response force from designated indentation displacement and frequency in order to understand the elasticity of the tissue. The focus of this study is to develop a finite element model to interpret the data collected by the EVE device and understand the tissue dynamics.

1.3. Goals and Approach

The main goal of this investigation is to develop a finite element model to interpret the data obtained through the EVE device and further understand the behavior of human vaginal tissue. Abaqus FEA 6.13.3 was used to simulate the interaction between EVE and the test material of either phantom tissue or biological tissue, then characterize the mechanical properties of the material.

The model was first validated using Hertz theory of elasticity. This theory was used to validate indentation testing of an elastic material with a spherical indenter. An assessment of the model

was then conducted comparing the data collected from EVE on a hydrogel phantom tissue with known elastic properties to the results generated by the simulation. The phantom tissues were developed by the Kieweg research team [M. Pacey] and tested with EVE. It is assumed that after congruency of the model with phantom data, the model can then be used to interpret *in vivo* data collected from human subjects. The model was also developed to further explore impacts from multiple layers of various tissue properties. This evaluation provides insight to the influence adjacent tissue has on the vaginal tissue structure which may be reflected in future *in vivo* experimental data.

1.4. Tissue Characterization

Vaginal tissue is a complex, multi-layer tissue. It is commonly depicted as having three distinct layers: the vaginal mucosa, the vaginal wall, and the adventitial layer (Figure 1). The mucosa is the inner most layer lining the vaginal lumen. This layer varies in thickness from 15 to 200 micrometers as it sheds old cells and builds new cells depending on hormonal stimulations from the ovaries [4]. As the layer changes in thickness, the elasticity changes as well becoming most elastic when the layer is thickest. The vaginal lining is covered with rugae which are transverse ridges that allow the vaginal cavity to expand. The middle layer is the vaginal wall. It consists of two layers of muscle fibers. The layer closest to the mucosa consists of circular layers of muscle fibers. The outer layer consists of longitudinal layers of muscle fibers. Together these muscle fibers provide a thick, elastic wall of muscular tissue to allow for childbirth. Finally, the adventitial layer is the outer most layer of the vaginal tissue. It covers the vaginal wall and houses the nerve fibers, lymphatic ducts, and blood vessels needed for tissue function. This tissue layer also connects the vaginal tissue to its surrounding organ tissues such as the bladder and rectum as well as other pelvic tissue structures [5].

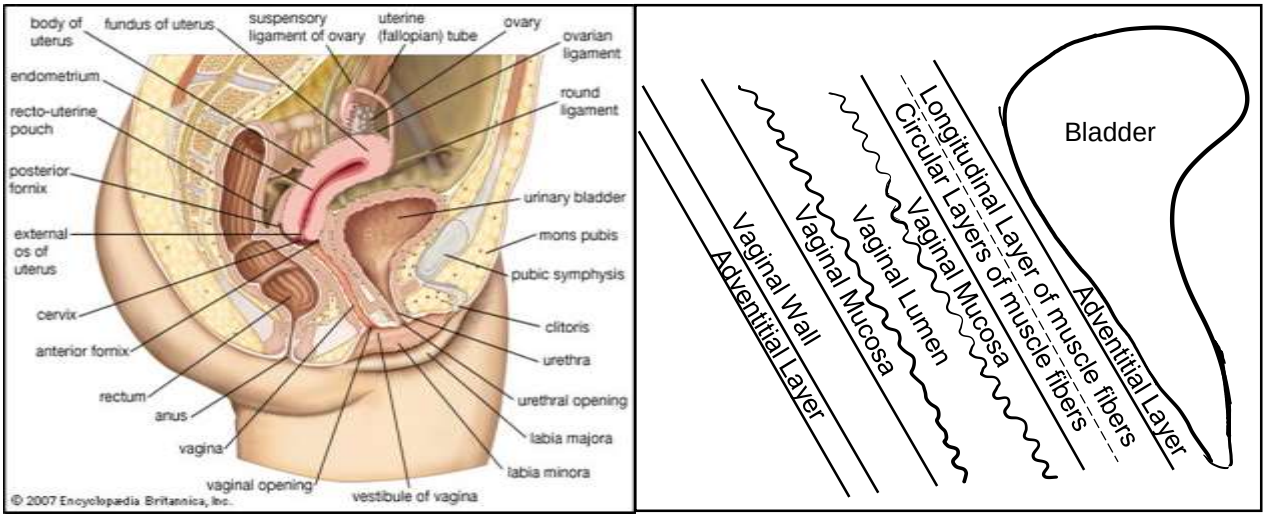

Figure 1: Female human anatomy in the sagittal plane (Left) and schematic of vaginal tissue layers not to scale (Right).

1.5. Review of Relevant Literature

Indentation testing is a common practice used to test for material properties. This form of testing has been used in the study of biological tissue properties as well. For various internal tissues (e.g. breast tissue, organ tissue, and vaginal tissue), evaluation is often conducted on excised tissue. Because of this, tissue is typically diseased and in the process of corrective surgery. Healthy tissue may be studied as well and is generally cadaveric tissue. During testing, the tissue sample is compressed using a mechanical indenter instrument which can vary in shape from a flat-ended cylindrical punch to a round hemispherical shape to a cone shape. The indentation device is prescribed a maximum displacement at a specified rate, and the corresponding force measurement is determined. The indenter shape can cause a difference in the force response due to the contact area [6, 7]. Additionally, variations of this test can be completed with monotonic loading [8] or cyclic loading. In either case, the loads may be applied to rupture in order to determine properties such as Young's modulus and stress and strain values. In some cases, the response is expanded to show viscoelastic response. The Prony series has been used to express a second order, linear, viscoelastic model [9] and to characterize shear relaxation [10]. Other models such as the Fung model, which exponentially relates the strain

stiffening behavior expressed in the first strain invariant, and the Ogden model, which predicts large strain, have been shown to provide a better fit for biological tissues than other strain energy functions such as the Mooney-Rivlin, the reduced polynomial, and Van Der Waals [11]. In order to obtain an elastic modulus value from load displacement measurements, the Oliver-Pharr method has been used due to its high sensitivity to stiffness and insensitivity to indenter diameter and sample thickness[12].

Evaluating vaginal tissue, many of the published studies utilized tensile testing to characterize biomechanical properties. These tests must use excised tissue and perform cyclic loading to rupture. The tensile tests often reveal hyperelastic properties with nonlinear behavior [4, 13]. Many of these studies are the focus of prolapsed tissue research and therefore use diseased tissue excised during correctional surgeries. Again, comparative healthy tissue often comes from cadaveric tissue or may come from healthy tissue excised during hysterectomies removing the cervix. Since the elasticity was also found to vary with age [13], this could affect outcomes in comparisons with cadaver tissue depending on the age of the woman at time of death. Additionally, prolapsed tissue has also been found to be more extensible than healthy vaginal tissue [14]. More recent studies have attempted to test tissue *in vivo*. A hand-held tool was designed using motion tracking and pressure sensors to determine the elastic properties. As a result, the tissue had an elastic modulus range varying from 2 to 40 kilopascals and a reproduced accuracy of 20 percent within the range [15]. Other researchers have utilized Cutometers® to determine the elasticity. Prolapsed vaginal tissue was evaluated *in vivo* by the maximum uplift induced by the vacuum suction while patients underwent corrective surgical procedures [16].

While several different test methods and constitutive models have been used to define tissue mechanics, finite element analysis (FEA) has also been used in conjunction with indentation

testing of various types of tissue. FEA provides the ability to obtain properties that were unable to be determined directly from the indentation test data. Poisson's ratio has been determined by utilizing the finite element model with different size indenters. The FEA simulated force and displacement data sets for each indenter size were used to calculate both Poisson's ratio and Young's modulus [17, 18]. Many of the models were validated first with an elasticity theory such as Hertz theory of elasticity. FEA was then used to determine viscoelastic or hyperelastic behaviors [10]. After elastic validation, Arruda-Boyce constitutive law has been used to expand the initial estimate of breast tissue with very large strains to hyperelastic, nonlinear characteristics. Using mathematical iterations, the model was able to determine the elastic modulus to match the experimental data [19]. Alternatively, an iterative method was also used to calculate the elastic modulus with porcine liver tissue being compressed over different strain rates. With an initial local elastic modulus and Poisson's ratio estimated, the FEA values converged to two percent of the experimental value [20]. For time-independent elastic response, neo-Hookean has been utilized during simulation of liver tissue [6]. While several constitutive models have been used to model the response of a variety of tissues, the indentation test was simulated in two dimensions and defined as incompressible, isotropic, and homogeneous.

As is shown above, previous research has led to advancements in being able to measure tissue properties *in vivo*, calculating additional properties, and developing finite element models of the tested tissue. This has also led to further understanding of differences between normal and diseased tissue as well as how factors such as age affect the properties [14]. As the more recent literature suggests, it is important to study and understand the healthy tissue *in vivo* due to the broad range of elasticity values found in vaginal tissue as well as for comparison to determine the change in properties of diseased tissue. In addition, it is not clear from tensile testing or cutometry how underlying tissue may affect the dynamics of the vaginal tissue. Furthermore, Young's modulus has been shown to be significantly greater and overestimated when obtained from

tensile testing as opposed to indentation testing [21]. During the time period when the mucosa layer increases in thickness and elasticity, cutometry testing may only be evaluating the properties of the mucosa layer rather than the properties of the collective vaginal tissue layers. For these reasons, our studies have contributed by developing a new tool for the purpose of *in vivo* testing, developing a finite element model using Abaqus to simulate the three-dimensional dynamics in order to understand the mechanical properties of the tissue, and incorporating adjoining tissue to understand how underlying tissue impact the vaginal tissue properties.

While HIV has been the primary motivation in understanding the tissue mechanics, this knowledge can also be used in other areas. Other applications of vaginal drug delivery could also use this knowledge to develop drug delivery systems. In addition, medical devices used to correct prolapsed tissue could benefit from the new found knowledge. By having a more complete understanding of the characteristics of healthy tissue, improvements and new designs for medical devices to correct prolapsed tissue could emerge.

Although the work above has developed 2-dimensional mathematical models of tissue with the assumptions of homogenous, isotopic, and elastic or hyperelastic properties, the effects of layers with various elastic modulus values has not been explored. In addition, minimal experimental studies of healthy, *in vivo*, vaginal tissue have been conducted resulting in a broad range of elastic modulus values. While the previously published finite element analyses focus on interpreting single layer, 2-dimensional layers of other biological soft tissues, this study will allow interpretation of *in vivo* data three-dimensionally and identification of adjacent tissue effects on the force response of the vaginal tissue. It will also help interpret the *in vivo* data and identify if viscoelastic properties exist by evaluating force patterns corresponding to displacement of the tissue. In order to accomplish this, a mathematical model was developed using Abaqus 6.13.3 to simulate displacement with iterations of mechanical properties to provide force and stress output.

This model was then validated using Hertz theory of elasticity and compared to experimental data from hydrogels with known properties.

The model was developed to interpret the vaginal tissue response during *in vivo* indentation testing while applying multiple layers to the tissue to see additional effects. It is our hypothesis that a finite element model will provide a more complete interpretation of EVE data than using the "direct" estimate of E from oscillatory force-displacement data. Previous studies from Oyen [7], Samur [10], and Martins [4] have shown the use of FE to obtain mechanical properties of materials that were unable to be obtained through indentation testing alone. They have also shown how an FE model can be employed to gather additional data and information rather than going through more experimental work.

Collective evidence reviewed in this section strongly supports the conclusion that there is a need to more accurately identify material properties of human vaginal tissue. The understanding of these properties will aid in the development of drug delivery systems for the prevention of the spread of disease and in the development of medical devices for diseased or weakened tissue.

1.6. Significance

Understanding of material properties is critical in coating applications including bioengineering drug delivery systems. Utilization of finite element modeling for evaluating the mechanical properties of tissue has allowed for more complete understanding of the properties as well as allowing for additional testing through the model rather than experimentally.

While much analysis has been done on excised and diseased or prolapsed vaginal tissue, only a few studies have been done with healthy, *in vivo* tissue. In addition, most *ex vivo* testing is

done using tensile tests rather than indentation testing. The focus of those tests is for understanding the diminished tissue properties found in prolapsed tissue. Tensile testing can provide valuable insight on strength and elasticity properties, however the tissue cannot be tested *in vivo*. The *ex vivo* testing can cause a large variation in values as is currently seen among research groups. Tensile testing has also been found to result in higher elasticity properties than results determined from indentation testing [21]. The most common method of *in vivo* testing uses a vacuum chamber and cutometry to determine the displacement caused by the corresponding pressure. This method does not account for underlying muscles, fat, bone, tendons, or other adjacent tissues which can influence the natural mechanics of the tissue. In addition to testing, many studies have included finite element analyses. Previous models have utilized single layer, two-dimensional analysis. This type of model does not account for underlying tissue and assumes isotropic properties.

Increased understanding of the tissue properties has the possibility to effectively improve drug delivery mechanisms as well as product development for prolapsed tissue. It is anticipated that this research will provide a more complete interpretation of the data collected using an *in vivo* indentation device. The tissue mechanics of both the vaginal tissue and the underlying tissue were modeled for a comprehensive representation of *in vivo* effects. This provided an understanding of what is occurring throughout the tissue rather than a single data point. A three-dimensional model was developed to allow for the future incorporation of anisotropic properties, and multiple layers were also included to determine the effects of underlying tissue.

Through the development of an accurate model representation of healthy, *in vivo*, vaginal tissue, medical applications can emerge with new solutions and to further improve existing products. This development can impact applications such as product development for and

diagnosis of prolapsed tissue correction and drug delivery methods for vaginal infections for both preventive applications and medical treatment.

2. Methods

2.1. Introduction

As of 2013, 35 million people worldwide are living with HIV or AIDS [1]. Researchers are working to develop microbicides to fight this epidemic. These microbicides are designed to coat the vaginal or rectal canals and prevent the spread of HIV [1]. In 2010, the trial CAPRISA 004 evaluated the effectiveness of Tenofovir gel in women when applied before and after intercourse. The study showed the gel was able to reduce incidents of HIV spreading by 39 percent. The efficacy of gel microbicides depends partially on the ability to coat the epithelia of the vaginal tissue and partially on the ability to stay within the cavity without leakage. Understanding the mechanics of this tissue is crucial in determining how the gel flows over the epithelium mucosa layer. These are equally important in order to address the issue of acceptability by the user as was seen in the VOICE study [3, 22].

Vaginal tissue has been studied to understand the complex dynamic properties. With three distinct layers of tissue making up vaginal tissue, each layer is designed to change for various functions. The mucosa layer which lines the vaginal canal is an epithelial layer that changes in both thickness and elasticity as changes occur in hormone levels. The muscular vaginal wall is made up of both weak layered circular fibers and strong layered longitudinal fibers. This wall also changes in elasticity in order to allow for vaginal childbirth. The outer adventitial layer contains blood vessels, nerve fibers, and lymphatic ducts used in tissue function. This layer also is the connective tissue that adjoins vaginal tissue with surrounding tissue such as the bladder [5].

In order to determine tissue properties for further definition and understanding, various mechanical testing has been performed. Tensile tests are very common for testing vaginal tissue. Excised tissue samples are removed from the tissue in order to perform the test [4, 13, 14].

Because of this, the tissue is often prolapsed or diseased and removed during corrective surgery. Some studies have obtained healthy tissue samples from cadavers for comparison of tissue properties. While this testing can provide good insight in to the properties, accuracy of the values may be affected from testing the tissue *ex vivo*. Several factors can impact that data and cause variations including hydration, storage, temperature, and excision time.

More recently, Cutometry® has been used in order to test the tissue *in vivo*. This form of testing utilizes vacuum pressure to displace the tissue and determine elastic properties [16]. The ability to test *in vivo* tissue eliminates many external effects of the tissue. However, by applying a pull force, the impact of deeper underlying layers may not be present in the results particularly with the mucosa layer varying in thickness.

While indentation testing has been used to determine properties of various tissues, applying this technique to *in vivo* vaginal tissue has only been used once before. In this case, a hand held device was designed to perform the indentation testing including motion detection and pressure sensing to determine elasticity properties. The results produced a large range of values and an even broader range for reproducibility[15]. The hand held device leaves room for possible human errors during testing.

In addition to experimental testing, finite element analysis is used for data evaluation and in parallel with testing to perform additional evaluation through modeling. FEA can provide further understanding of the dynamics of the tissue as well as evaluate the data collected from experimental tests. Previous studies of various tissues have used two-dimensional, axisymmetric, single-layer models with isotropic and homogenous assumptions to simulate indentation of tissue [6, 10, 17, 19, 20].

The *overall aim* of this study was to develop a finite element model to accompany the EVE device previously designed by the Kieweg research group. With the device designed to perform indentation tests on phantom and *in vivo*, human, vaginal tissue, the purpose of the FE model was to interpret force-displacement data collected by EVE. The model was also used to determine impacts of adjacent tissue by varying stiffness of the underlying layer. Finally, the model is developed in three dimensions to allow for the addition of anisotropy.

2.2. Methods

Abaqus CAE 6.13.3 was used to develop and validate a finite element model simulating indentation of an elastic rectangular prism with a rigid spherical indenter.

2.2.1. Model Part Definition

2.2.1.1. Spherical Indenter

The spherical indenter was defined as a three-dimensional, analytic, rigid shell with a 9.65 millimeter radius. Because the indenter was much stiffer than the tissue, modeling the part in this way allows the deformation of the indenter to be neglected. By defining the part as analytic, it was also less computationally expensive. The sphere was given the dimensions of the indenting hemisphere located on the EVE device.

2.2.1.2. Rectangular Prism/Tissue

The tissue was modeled as an extruded solid, rectangular prism. The prism was given dimensions of 60 millimeters in length, 30 millimeter in width, and 20 millimeters in thickness or depth based on measured values [23]. Due to symmetry, the part was then partitioned to represent a one-quarter quadrant of the tissue, and one corner was defined as the tissue center (Figure 2). The mesh seeds were manually defined in sections with the number of seeds decreasing away from the tissue corner designated as the tissue center (Figure 3). The seeds

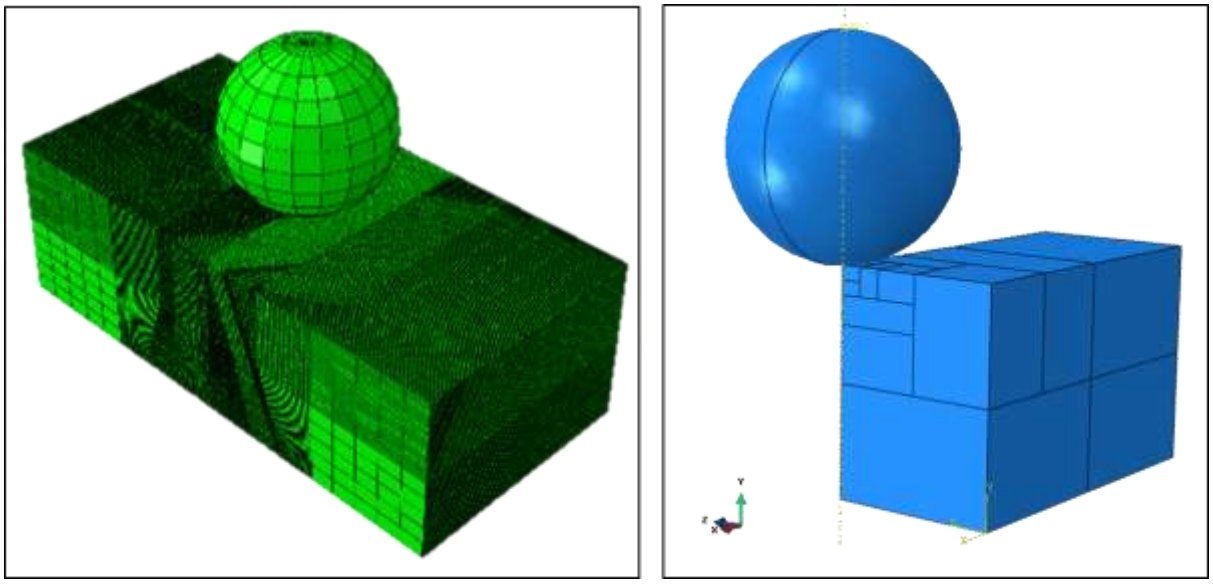

Figure 2: Tissue and spherical indenter assembly. (Left) Full tissue shown with indenter located in the center. (Right) Partitioned quadrant with indenter located on the corner depicted as tissue center.

were constrained to allow for the number of elements to increase only. The mesh shape was defined as hexagonal and applied with a sweeping technique with an advancing front. This allowed the mesh to remain hexagonal throughout the part. The region of the tissue with the finest mesh was defined with mesh element types C3D8R. This classified the region as 8-node

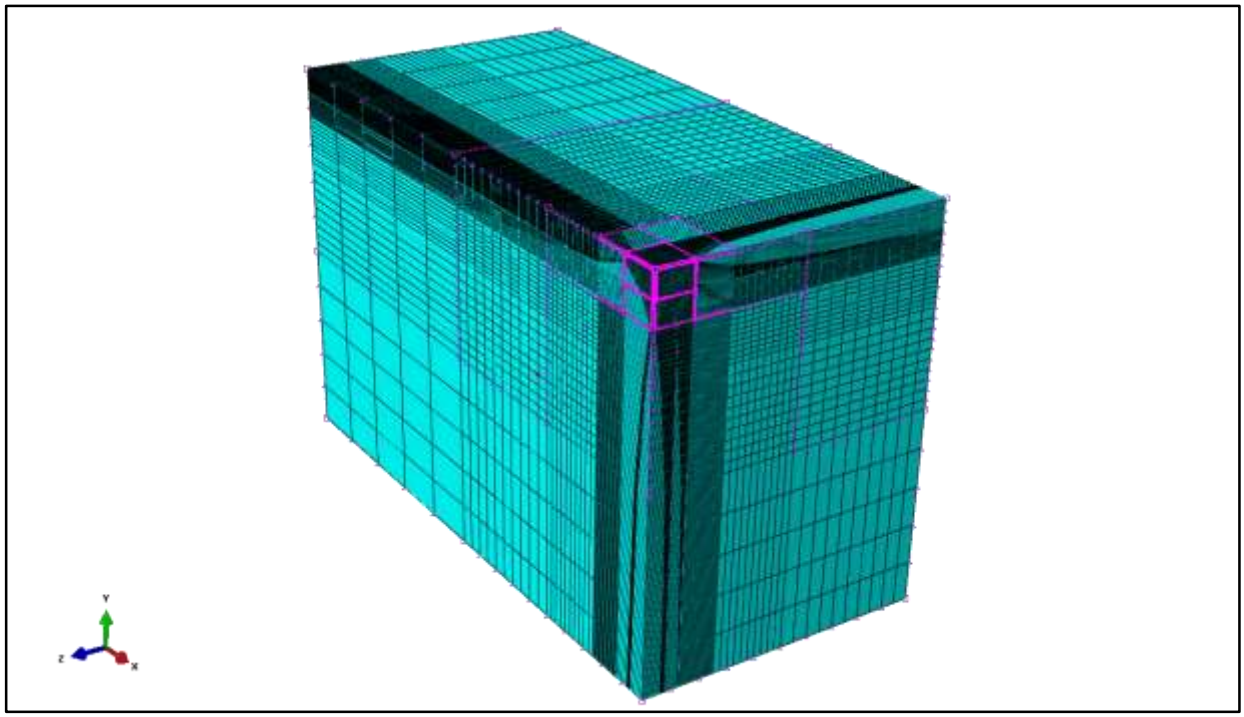

Figure 3: Tissue quadrant with sweeping mesh.

bricks with reduced integration (uses Gaussian Quadrature and evaluates the material response at each integration point in each element) and hourglass control. Further, the region was characterized as being a continuum solid with three degrees of freedom.

Once the part was defined, three constraints were applied. First, the face in the X-Y plane was made symmetric in the Z direction (Figure 4A). Similarly, the face in the Y-Z plane was made symmetric in the X direction (Figure 4B). These constraints were necessary due to the partitioning of the part to one-quarter of the original size. The bottom face of the part was constrained in the Y direction. This was necessary to understand the response forces in the tissue during indentation. Finally, the tissue was given initial material properties with a Young's modulus of 7.4 kPa and a Poisson's ratio of 0.48. These values were average values of vaginal tissue properties previously found in a study by Egorov [15]. The density was defined as 1.06 kilograms per liter, the average density of skeletal muscle [24]. For initial evaluation and validation, the tissue was characterized as elastic, homogenous, and isotropic.

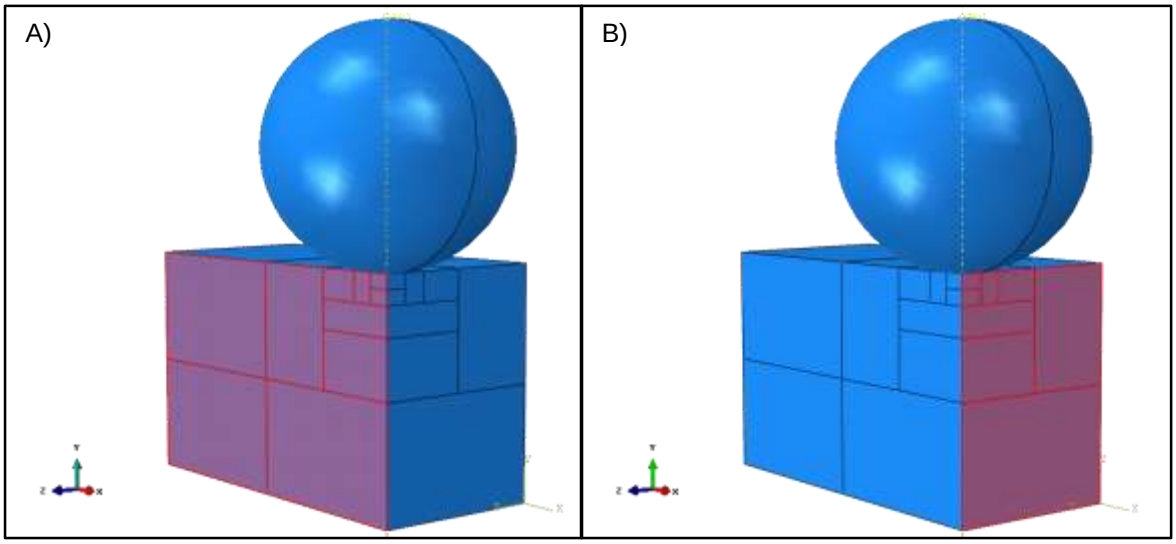

Figure 4: (A) Constraint applied to X-Y plane for symmetry in the Z direction (B) Constraint applied to the Y-Z plane for symmetry in the X direction.

For the evaluation of influence from underlying tissue, the tissue part was divided horizontally. The top 7 millimeters were defined as listed above. The lower 13 millimeters were varied in elasticity in order to evaluate possible influence surrounding tissue may have on the vaginal tissue testing *in vivo*. The interface between the layers was continuous with no sliding effects.

2.2.1.3. Assembly

Instances are copies of the defined parts required for assembling the parts together. The parts were copied as dependent instances and assembled such that the indenter is located at the corner defined as the center of the tissue. By defining the instances as dependent, changes made to either part will automatically be updated in the instance as well. The interaction between instances was characterized as surface-to-surface contact with the indenter defined as the “Master Surface” and the tissue as the “Slave Surface” using the kinematic contact method and finite sliding formulation. The contact interaction properties were defined as having frictionless tangential behavior and “Hard” contact for normal behavior.

2.2.2. Model Function and Validation

Once the parts were defined and the model assembled, the validation process followed. The indenter was prescribed to move from the zero position on the tissue surface to a specified distance into the tissue. The indenter motion was modeled as a dynamic, explicit step. By modeling the movement in this way, Abaqus was able to perform computations more efficiently while still maintaining consistency with large deformation. This is due to the use of central-

difference time integration rule and lumped mass matrix. Explicit also provided automatic type increments with a global stabilization estimator.

Once the model was defined, the job was created and a full analysis was completed for validation. The model was validated according to Hertz theory of elasticity. This was completed by displacing the indenter -0.00095 millimeters into the tissue. This value was used in order to meet a condition needed to satisfy Hertz theory of elasticity which states that the contact radius must be much less than the relative radius of curvature. This ensures that the boundaries do not influence the stress field and that the strains satisfy the linear theory of elasticity [25]. In this case, the contact radius of 0.096 millimeters was selected such that it is less than 1 percent of the indenter radius of curvature. While this displacement is very small compared to the simulated indentation test, Hertz theory of elasticity is commonly used as the validation method. Because there is no large deformation analytical solution for validation, assumptions are made that the model satisfying Hertz theory will provide solutions for large displacement as well given the other conditions are satisfied. These other conditions implemented in order to satisfy Hertz theory include the surfaces defined as continuous, nonconforming, and frictionless. The strains were assumed to be small, and each solid could be considered an elastic half-space. The model was validated for two elastic modulus values. The values of 7.4kPa and 50kPa were used to show validity over a broad range. The calculations for Hertz Elastic Contact Theory can be found in Appendix I – Hertz [25].

2.2.3. Mesh Convergence

Upon validation, a mesh convergence study was completed for the Young's modulus of 7.4kPa. This value was chosen to minimize computation time. Also, from previously published studies by Egorov, this value is expected to be similar to the vaginal tissue elastic modulus [15].

The model mesh was refined by increasing the number of elements in order to increase the accuracy of the model. Five separate runs were completed with the initial run beginning with 20 x 20 x 10 seeding and increasing the number of seeds by 10 on each dimension for each run (Figure 5). This increase was only performed on the section in contact with the indenter however was propagated through the tissue as seen in Figure 3. In addition to the mesh convergence study at small deformation (which could be compared to the Hertz analytical solution), a second convergence study was conducted at large deformations as well. This comparison was done with the same mesh values as the small deflections mesh comparison.

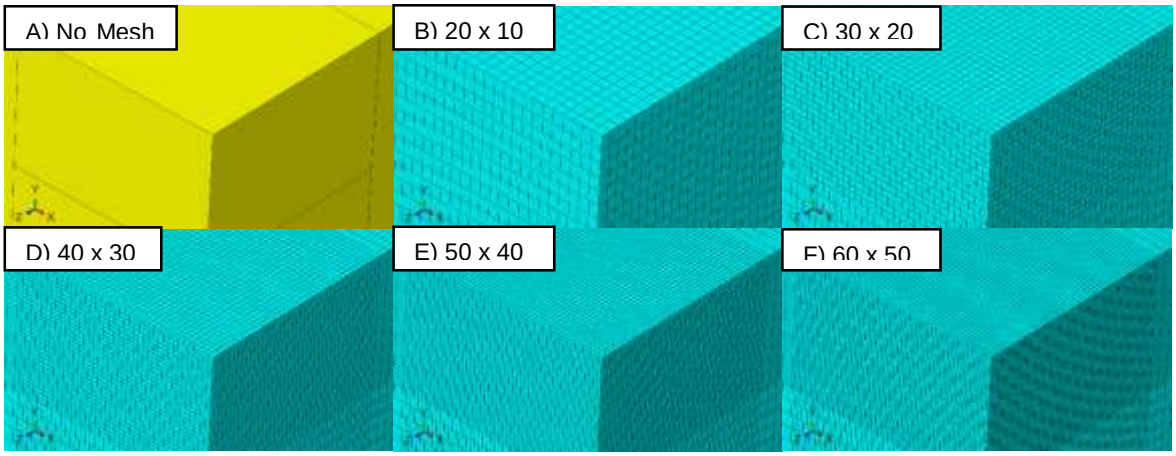

Figure 5: Zoomed view of meshed corner. This shows the changes in mesh as the number of seeds was increased. The numbers on each image indicate the number of seeds. The first number is the number of seeds in the X and Z directions (width) and the second number is the number of seeds in the Y direction (height). The seeding was changing in this partitioned cube and propagated through the part.

2.2.4. Simulation of Large Deformation of Single Layer Tissue

With the model validated for small indentations and the mesh size selected, evaluation of large indentation was conducted. The Young's modulus used in the model was selected from the previously published values as determined by Egorov's research group. Simulating one possible scenario of the compression of EVE experimental tests, the spherical indenter was prescribed to move -5 millimeters into the tissue. The force-displacement values were then evaluated along with the stress and strain effects throughout the tissue.

The simulated values were also evaluated against preliminary EVE experimental data collected from a phantom tissue. Since EVE utilizes oscillatory methods for collecting force-displacement data and the simulation uses a single displacement, the data from the 20th oscillation of the EVE experiment was used for this assessment. Other fundamental differences should also be noted including the geometry of the phantom compared to the simulated tissue. The phantom was created as a cubic block with cylindrical cavity unlike the flat tissue that was created in the simulation. Once inserted, the EVE device at the "zero" position caused an initial displacement of the phantom tissue of approximately 6 millimeters. EVE then performed oscillations displacing the phantom tissue an additional 1 and 5 millimeters. The FE simulation begins at a zero position and displaced 5 millimeters with no preloading. The displacement differences led to a simulation extending the displacement to 8 millimeters for comparison between the simulated data endpoint and the experimental data starting point.

In order to better determine congruency between EVE and the FE model, a flat phantom tissue with the dimensions of the simulated vaginal tissue could be created and experimented upon with EVE at a zero to 5 millimeter deflection. The FE model can then be used in a manually iterative method to vary the Young's Modulus and match the results obtained from the FEA with the experimental results. This process can be done in order to evaluate *in vivo* data as well. Nominal stress and strain values calculated from EVE data can eventually be used to automate the calculation in the elastic properties in the FE model specifically if hyperelastic properties are found during *in vivo* testing. This will be discussed further in the Future Work section

2.2.5. Simulation of Large Deformation of Multiple Layers

Once the single layer tissue evaluation was complete, a second analysis was performed. In this investigation, the top 7 millimeters of the tissue representing vaginal tissue [26] were held constant while the material properties of the lower 13 millimeters of the tissue representing

underlying tissue were varied. Three values were compared: 7.4 kPa, 20 kPa, and 50 kPa. Force-displacement values were compared as well as stress values. The displacement remained the same at 5 millimeters into the tissue.

Both analyses provided valuable understanding of how to interpret EVE measurements of the tissue. The single layer evaluation provided further understanding of the movement of the tissue as well as additional information of stress and strain properties. The multiple layer evaluation provided further insight on how the tissue may be influenced by various surrounding tissues.

3. Results and Discussion

3.1. Model Validation and Mesh Convergence

Force versus displacement plots were created in order to compare FEA model results to the Hertz theory of elasticity calculated results in order to validate the model (Figure 6). The model indenter was displaced 0.00095 millimeters into the tissue. The tissue was defined with an elastic modulus of 7.4 kilopascals, a Poisson's Ratio of 0.48, and a density value of 1.06 kilograms per liter. A comparison of the maximum force was completed using the average of the last 20 data points which included displacement values greater than 0.00094 millimeters. The average maximum force calculated by Hertz theory of elasticity was 0.00156 milliNewtons (mN). The maximum force calculated using FEA was 0.001096 mN. This is a difference of 5.2 percent.

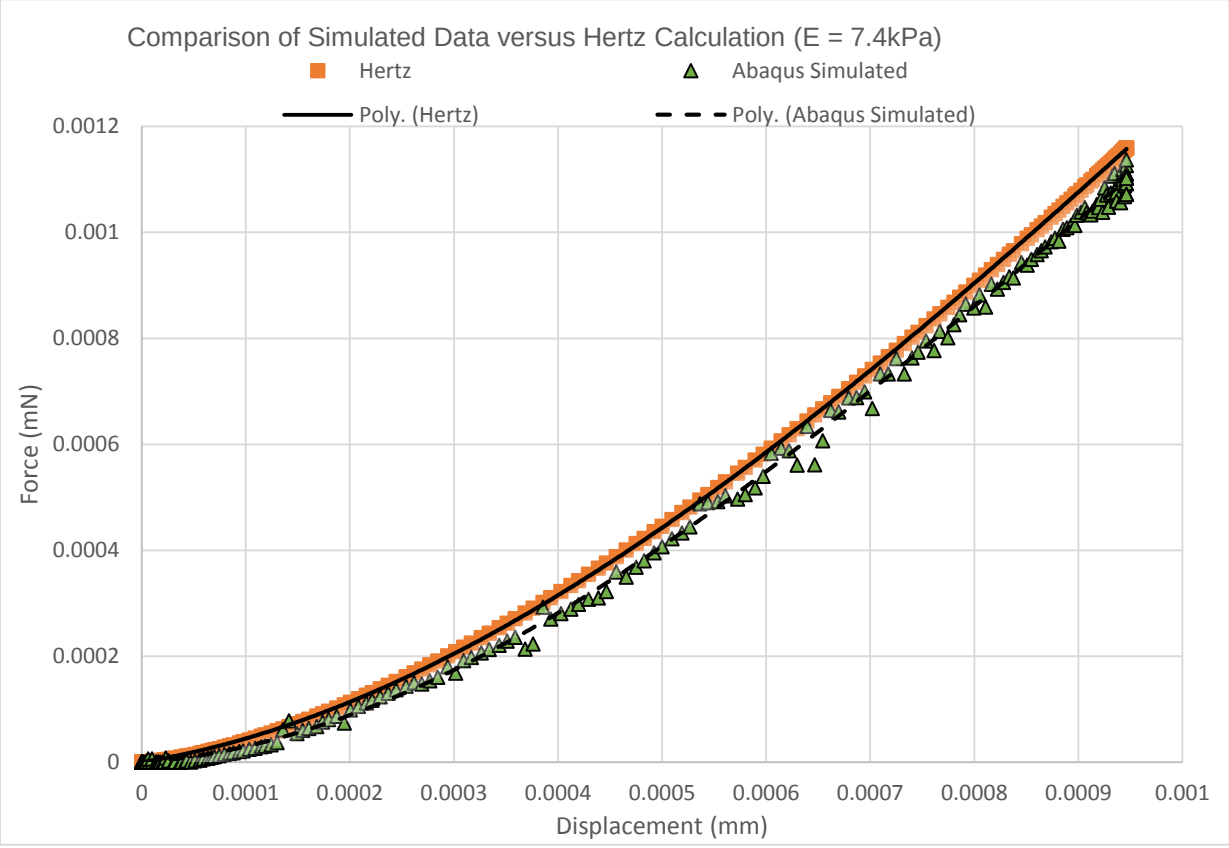

Figure 6: Force vs. Displacement plot comparison of Hertz theory of elasticity calculated results and FEA results at E=7.4 kPa.

A second evaluation was completed comparing Hertz theory calculated results with FEA results with elastic modulus values at 50kPa (Figure 7). Again, the comparison of the maximum force was done of the last 21 data points which included all points equal to or greater than 0.00095 millimeters. The FEA maximum force was 0.007919 mN and the Hertz theory maximum force was calculated to be 0.007976 mN. This was a difference of 0.78 percent. With the exception of a few outliers, again the FEA results align with the Hertz theory results. The outliers were part of numerical error during calculation. It is important to note that since the data was calculated for a single quadrant and then multiplied by 4, the outlier values were also quadrupled which may cause an exaggeration of the error rather than reflecting the true numerical error.

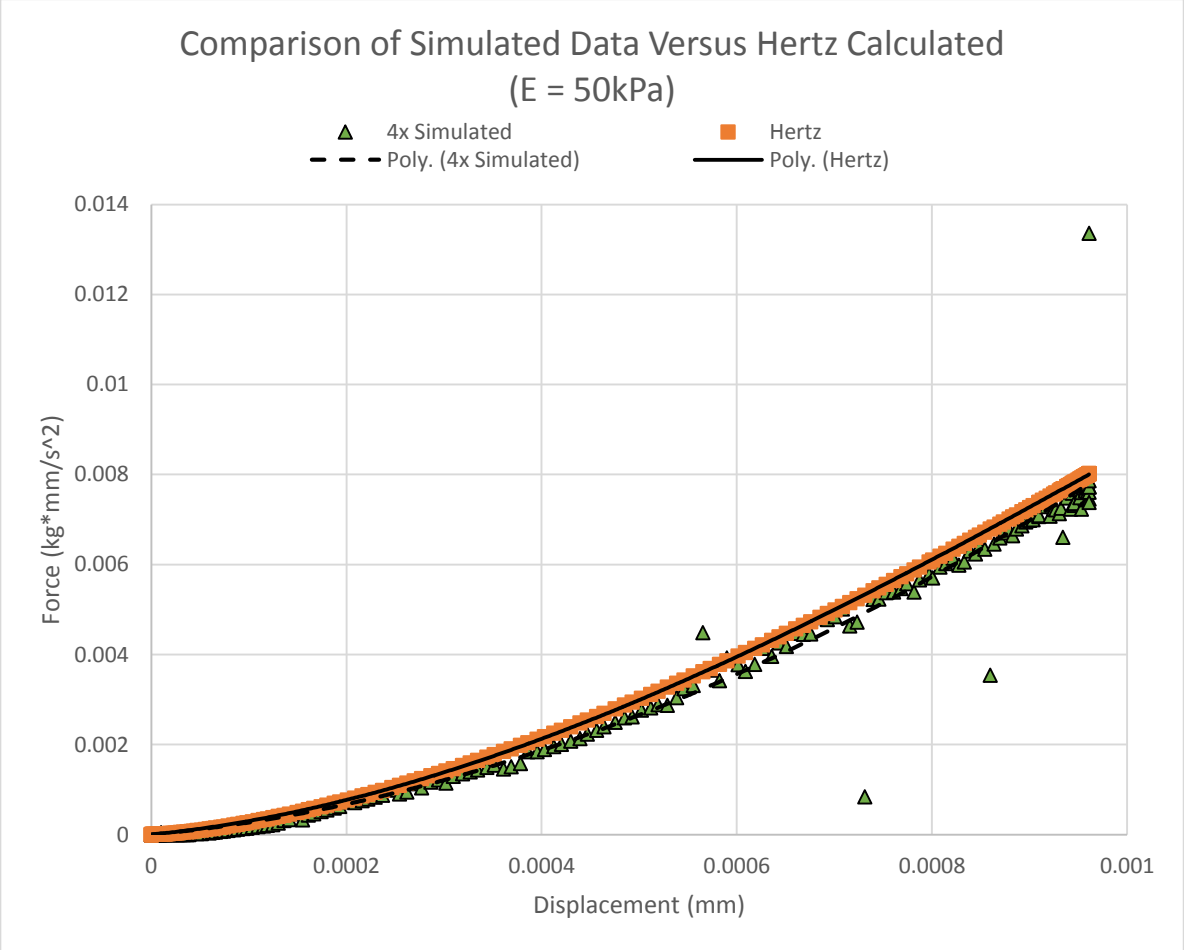

Figure 7: Force vs. Displacement plot comparison of Hertz theory of elasticity calculated results and FEA results at E=50 kPa.

With the model validated at small displacements, the mesh convergence study of the tissue was completed. The impact of the mesh sizes is prominent, however the values at all mesh sizes still followed closely to the Hertz calculated values (Figure 8).

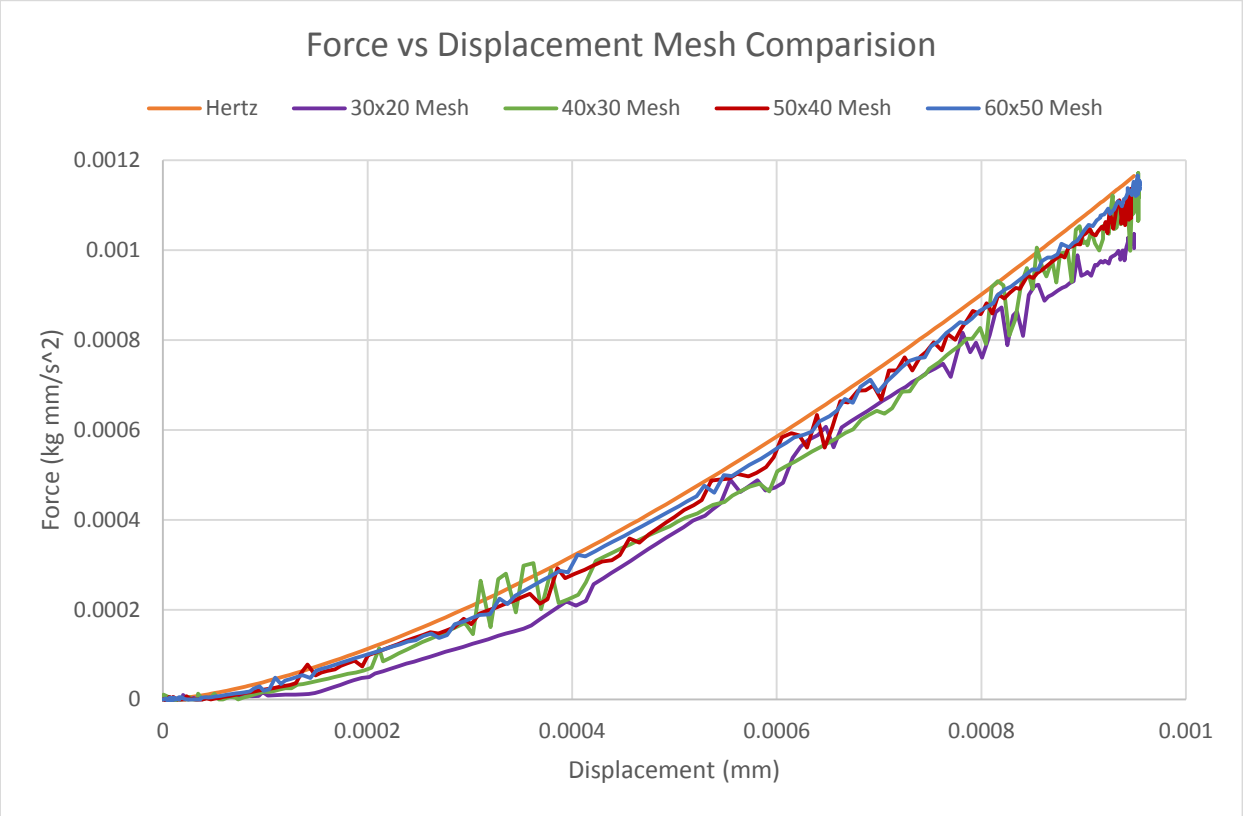

Figure 8: Mesh convergence plot for displacement of 0.00095 millimeters.

Table 1: Mesh comparison of small deformation showing convergence to Hertz value as mesh seeding is increased.

# Seeds (Width)	# Seeds (Height)	Run Time (Hours)	Distance (mm)	¼ Tissue Force (mN)	Full Tissue Force (mN)	Hertz (mN)	%Diff @max
60	50	28.6	0.000949	0.000288	0.001152	0.001164	1.053263
50	40	16.5	0.000946	0.000284	0.001137	0.001159	1.893975
40	30	13	0.000948	0.000282	0.001129	0.001162	2.892491
30	20	5.6	0.000949	0.000259	0.001035	0.001164	11.08536

Once validated and mesh convergence confirmed for small deformations, a mesh convergence was conducted for large deformations. When the force values were obtained from the different mesh sizes and compared to each other, the differences were less than 0.05

percent. This can be seen in Table 2 as well as in Figure 9 and Figure 10. Due to the computational time while still providing force response data similar to the finer mesh, the 30x20 mesh was selected for use.

Table 2: Mesh comparison for large deformation.

# Seeds (Width)	# Seeds (Height)	Run Time (Hours)	Distance (mm)	¼ Tissue Force (mN)	Full Tissue Force (mN)	% Diff to next mesh
60	50	72	4.98516	101.63	406.52	-0.04231
50	40	36.3	4.98586	101.673	406.692	-0.02656
40	30	21	4.98587	101.7	406.8	0.044248
30	20	5.3	4.98687	101.655	406.62	0.033446
20	10	4	4.98523	101.621	406.484	N/A

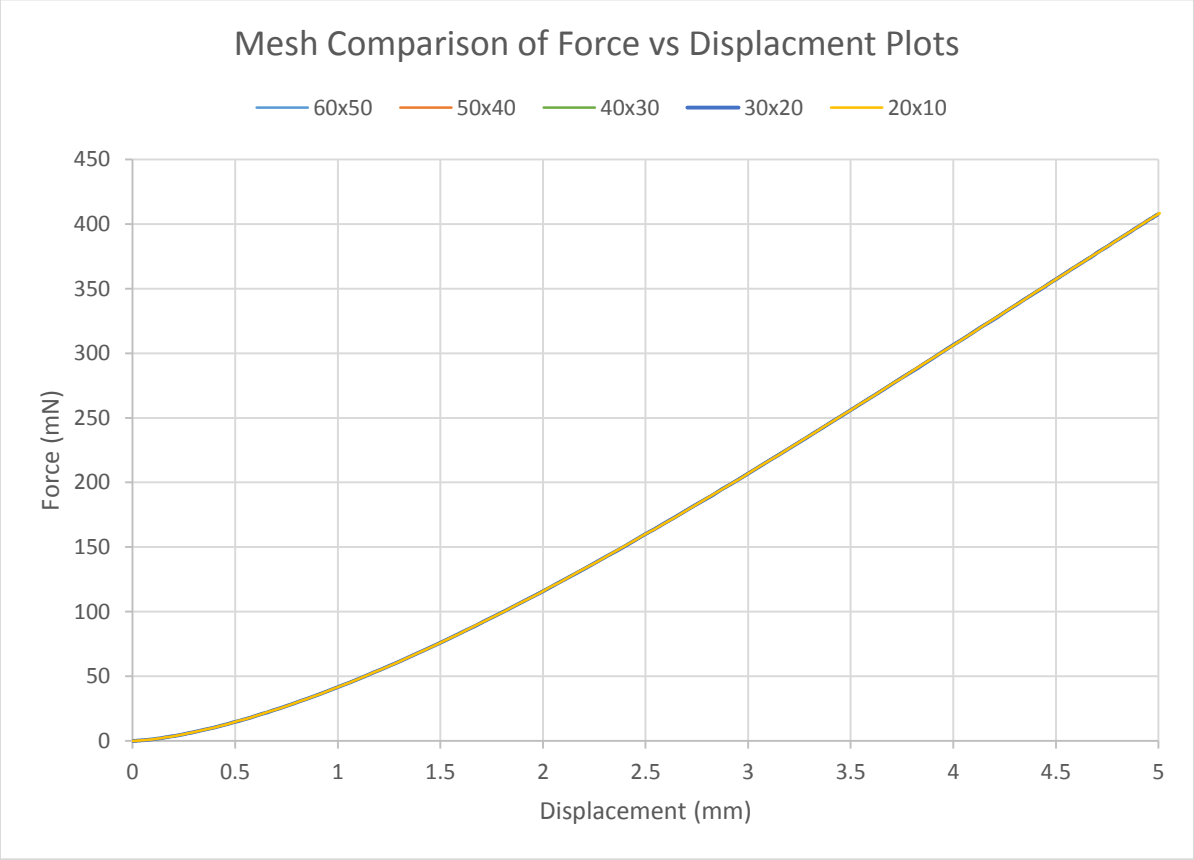

Figure 9: Mesh comparison plot of force versus displacement.

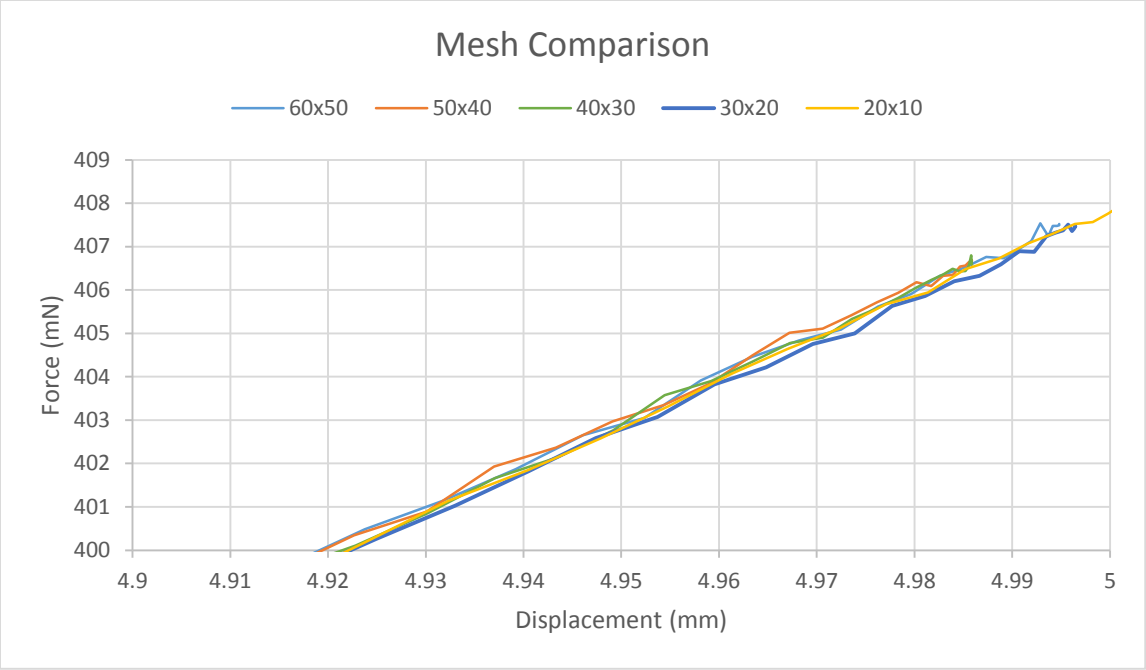

Figure 10: Mesh comparison plots of last 0.1 millimeter of movement into the tissue. This shows a clearer differentiation of each plot while still demonstrating the closeness in values.

3.2. Single Layer, Large Deformation Simulation

With the mesh convergence confirmed for large deformations, the simulation was evaluated at 5 millimeter indentation into the tissue with 7.4 kPa elasticity. The maximum resulting force was calculated at 0.4 Newtons. At smaller deformations, the force increases nonlinearly. After approximately 1 millimeter, the force increases more linearly with displacement (Figure 11). The contour plot of the displacement (Figure 12A) shows the impact of compression is much further than the prescribed displacement of the indenter. Impact in the Y direction is shown to influence as far as 17 millimeters from the top of the tissue. In the Z direction, the impact is through the entire 15-millimeter width of the tissue, while in the X direction, it is influenced approximately 10 millimeters into the tissue.

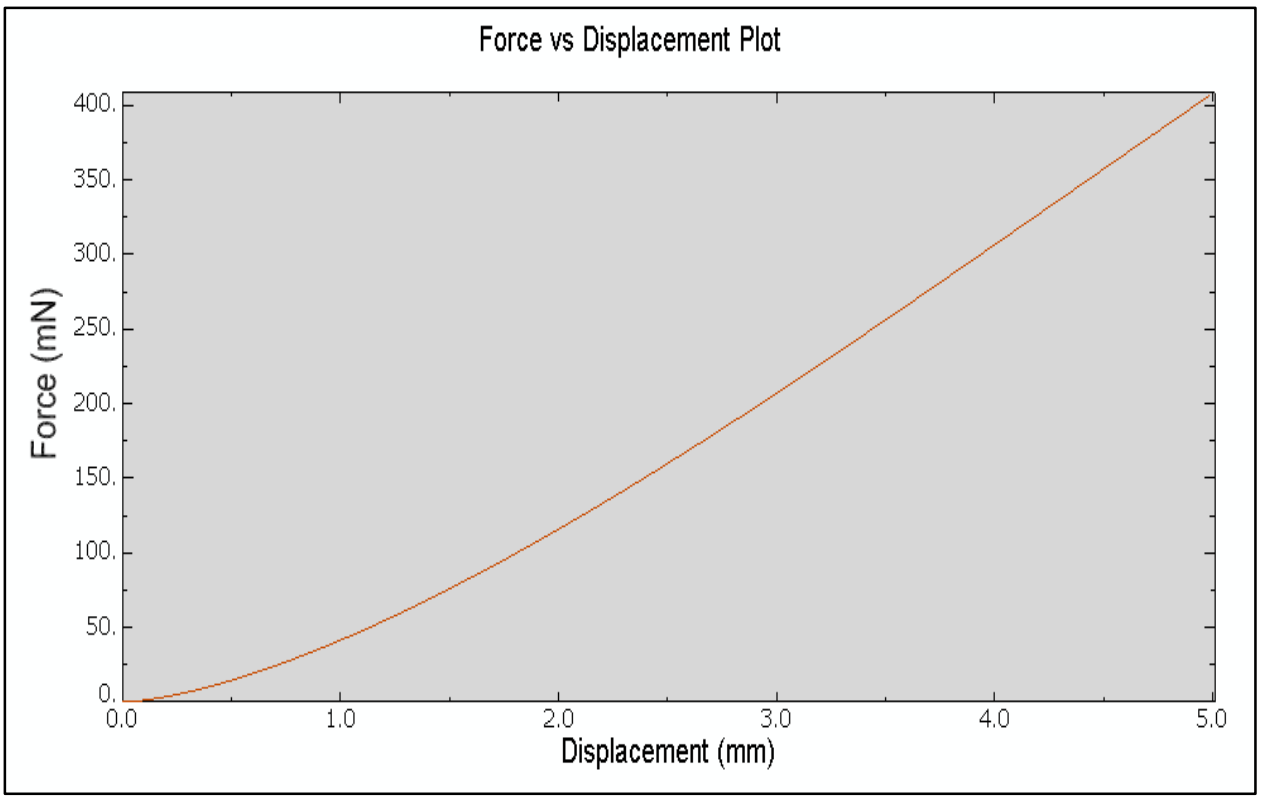

Figure 11: Force versus displacement plot of indentation simulation. Indenter moved 5 millimeters into the tissue.

Stress and strain contour plots were then evaluated. The maximum principle strain was calculated to be 0.8337 for the quadrant equating to 3.33 for the full tissue (Figure 12B). The von Mises stress was calculated to be 6.174 kPa for the quadrant equating to 24.69 kPa (Figure 12C). The maximum principle stress for the quadrant was calculated to be 6.16 kPa equating to 24.64 kPa for the full tissue (Figure 12D). The resulting stress and strain values are dominated by the stress and strain in the Y direction. Additionally, both the max principal stress and max principal strain can be seen propagating through the depth of the tissue with the maximum of these values located at the maximum deflection point.

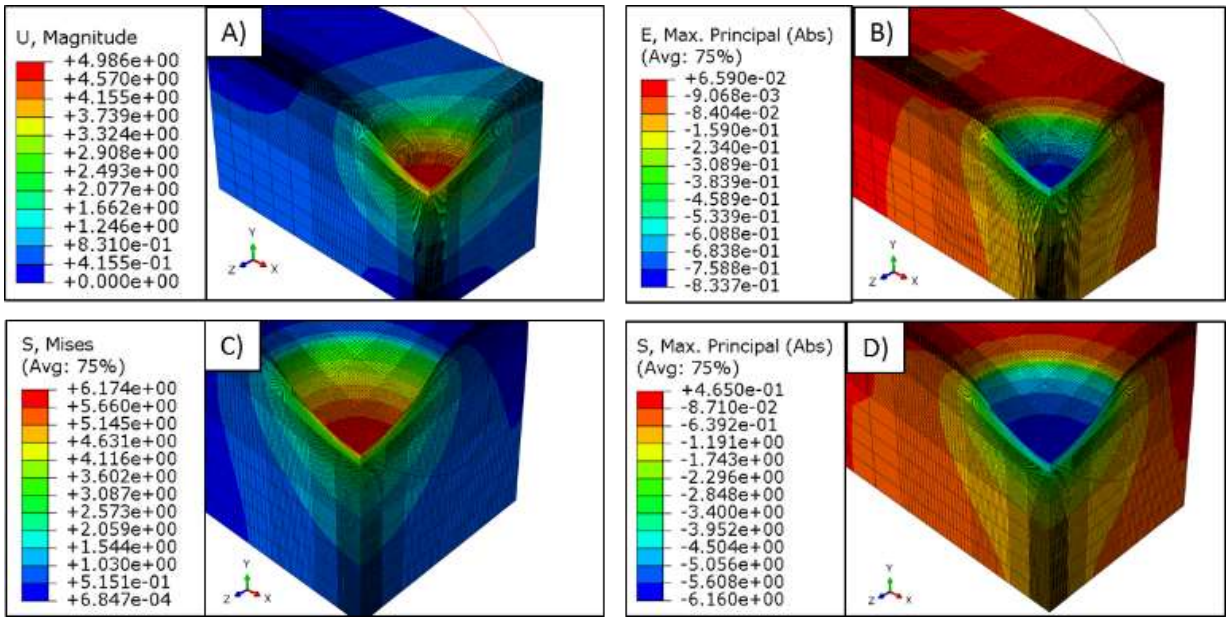

Figure 12: Contour plots of tissue after 5mm displacement of tissue with elasticity of 7.4 kPa. Note that all scales are specific to each plot. (A) Displacement plot showing movement of tissue caused by spherical indentation. (B)Strain plot showing propagation of strain through the thickness of the tissue and Z direction. Minimal strain through ¾ of tissue in Z direction. (C) Mises equivalent stress shows minimal stress through the thickness of the tissue with more significant stress occurring in the upper ¾ of the tissue. (D) Max principal stress proliferated through the entire thickness of the tissue after the deformation of 5 mm.

Comparing principal stress versus principal strain shows a near parabolic function which becomes approximately linear as the strain increases (Figure 13). Calculating the stress over strain values at each data point showed a convergence to 7.4 kPa reflecting the elastic properties as defined in the model. The nonlinearity is due to the nonlinear increase in contact area as the spherical indenter compresses further into the tissue.

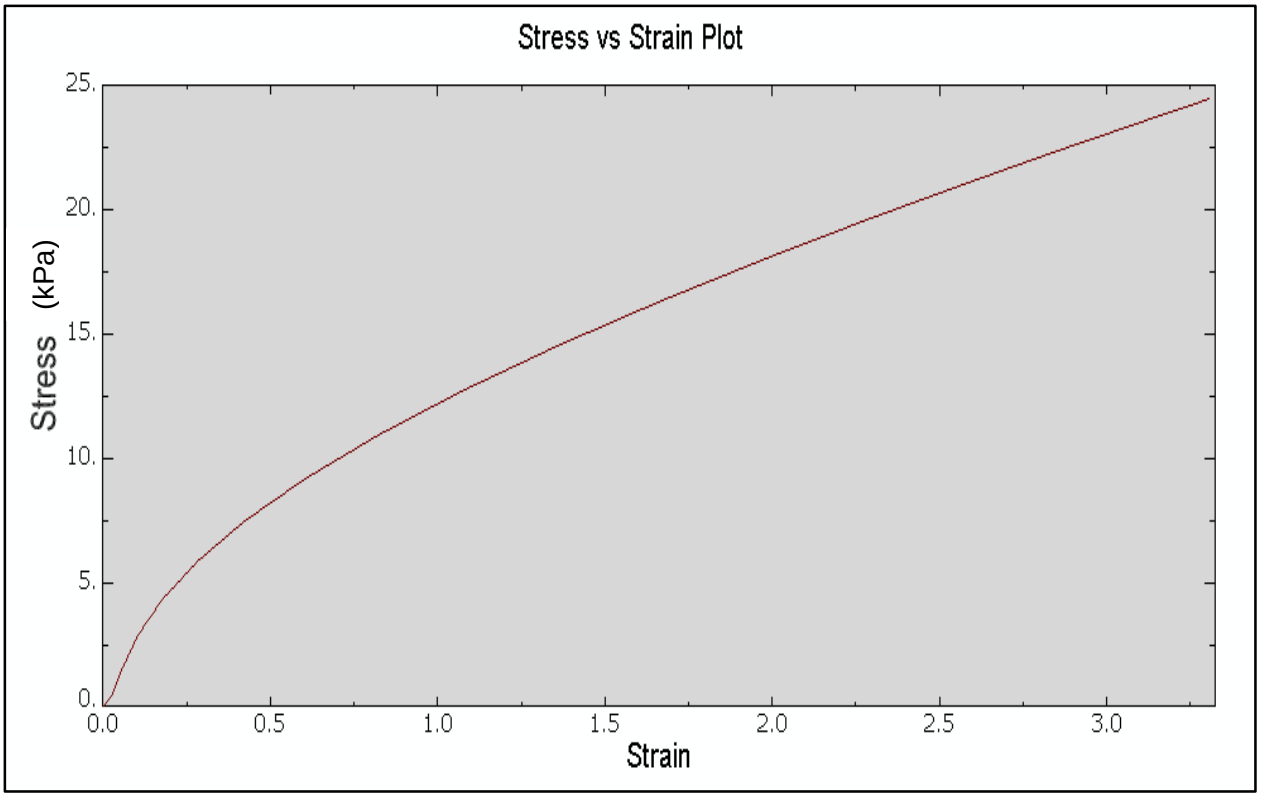

Figure 13: Stress versus strain plot. At maximum stress and strain, the elastic modulus is equal to 7.4 kilopascals.

3.3. Interpretation of EVE Data on Phantom Tissue

Comparison to preliminary EVE experimental data from phantom tissue was performed. Contrast between the two data sets demonstrated that the simulation did not completely replicate the influences seen during the phantom experimentation (Figure 14). In addition to slope differences, preliminary EVE data showed noise and a drift. After careful consideration, geometric differences also played a large role in the incongruent values. The EVE device fit snuggly when placed in a cylindrical cavity in the phantom tissue. This caused an initial displacement of approximately 6 millimeters from the indenter surface in addition to the pre-displacement of an additional 1 millimeter prior to the test displacement oscillation between 1 and 5 millimeters. This additional 7 millimeters of displacement along with the cylindrical shaped are believed to have contributed to the additional forces. This is due to the circumferential stress and strain caused by the phantom tissue wrapping around the probe end indenter. In addition to the geometric

difference, the displacement of the indenter beyond the 9.65 millimeter radius will cause a change in the tissue from non-conforming contact to conforming contact. When the deflection of the simulation was extended to 8 millimeters, the maximum force of the simulation at 8 millimeters was calculated at 0.838 N. This value is nearing the force of approximately 0.9 N calculated by the EVE device at an 8 millimeter deflection which included the 6 millimeter displacement caused by the insertion of the EVE device into the cavity. This force was an estimated average calculated because the noise that would not allow for an exact value. Finally,

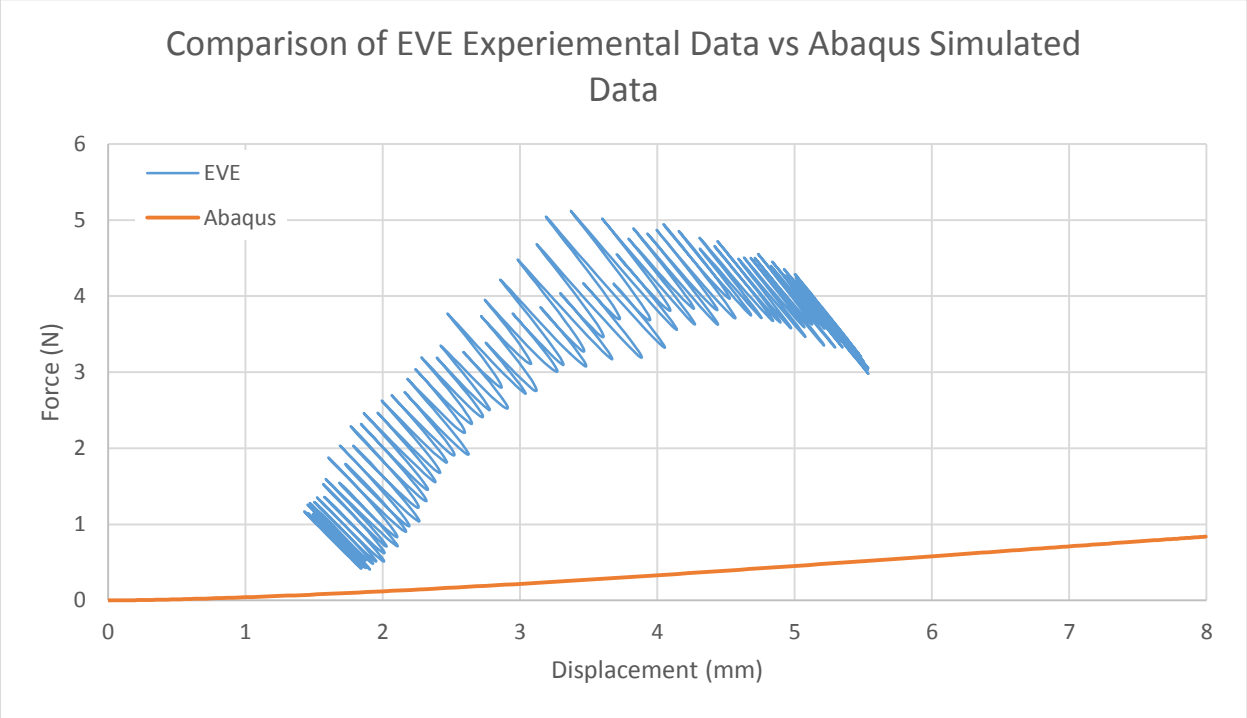

Figure 14: Comparison plots of force-displacement data for preliminary EVE experimental data on phantom and Abaqus simulated data. EVE plot shows the 20th cycle oscillation and does not include initial 6 mm deformation caused by insertion into the phantom. EVE data also contains noise which caused the spikes throughout the data.

3.4. Multiple Layer, Large Deformation Simulation

Upon completion of single layer assessment, the secondary model with variation in underlying tissue elasticity was evaluated to determine any influence this tissue may project on

the vaginal tissue during indentation experimentation. Five separate simulations were completed with variations in elastic modulus as listed in Table 3.

Simulation #	1	2	3	4	5
Vaginal Tissue E value [kPa] (Top 7 mm)	7.4	7.4	7.4	20	50
Underlying Tissue E value [kPa] (Lower 13 mm)	7.4	20	50	20	50

Table 3: Combination of elastic moduli for each of the five simulations performed. All values are in kPa. The top tissue contains the surface which is indented.

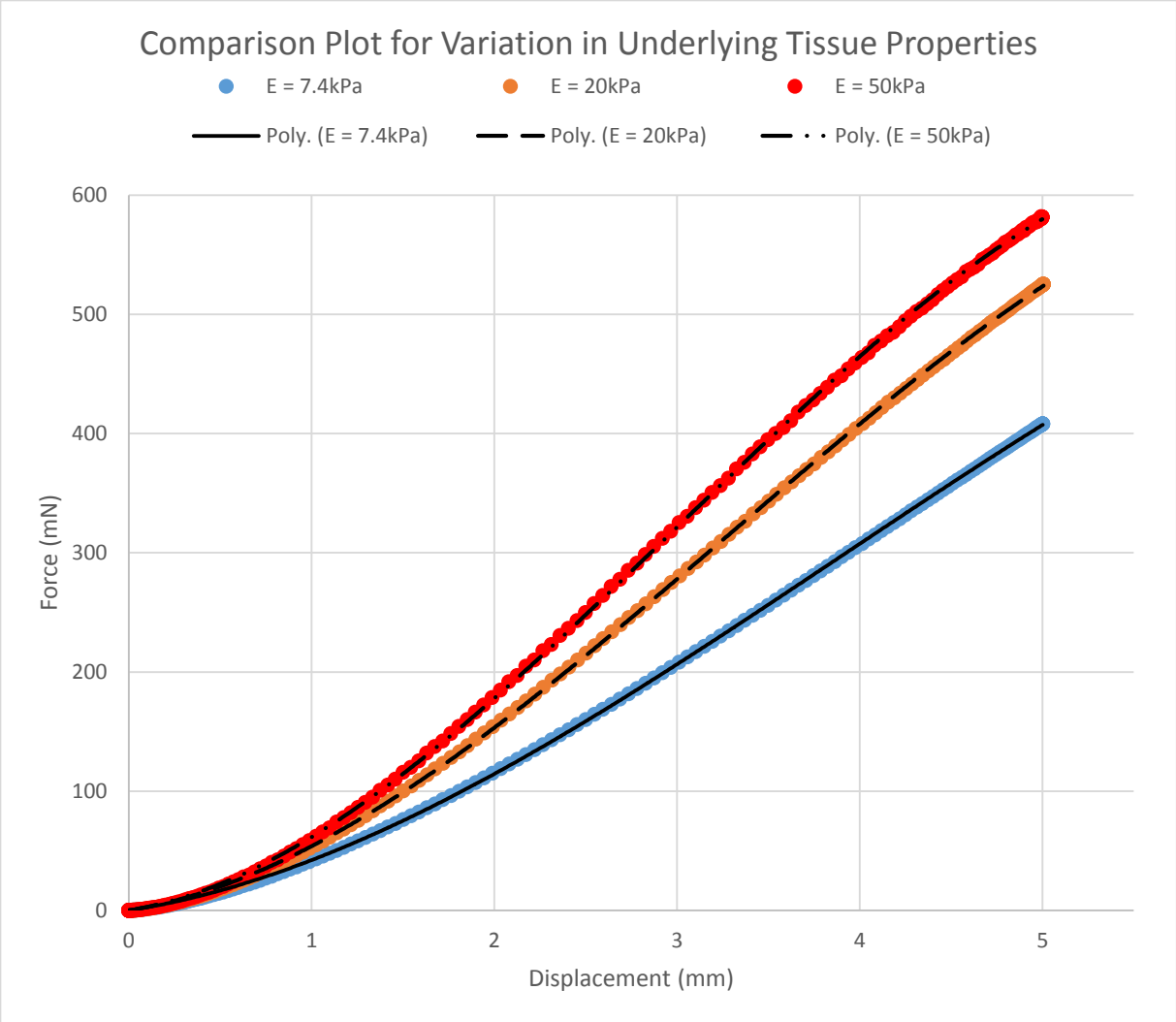

Figure 15: Comparison of multiple layer tissue with variation in lower tissue elastic modulus and a constant 7.4 kPa elastic modulus on the upper tissue (Siumaltion 1,2, and 3).

Impact from the underlying tissue is evident when comparing force-displacement plots. As the elastic modulus of the underlying tissue increases, the force required to move the indenter 5 millimeters also increase (Figure 15). However, the vaginal tissue elastic modulus (upper layer) provides the majority of the effect of the force. This is apparent when comparison is done against simulations with higher modulus values at the vaginal tissue as well as the underlying tissue (Figure 16). While the slopes of each curve were different, the change in the slopes were also different. For the plots with underlying tissue stiffer than that of the upper tissue layer, the slope of the plot increased and then decreased again at higher displacement. This change in slope can help identify stiffer tissue influences impacting *in vivo* measurements.

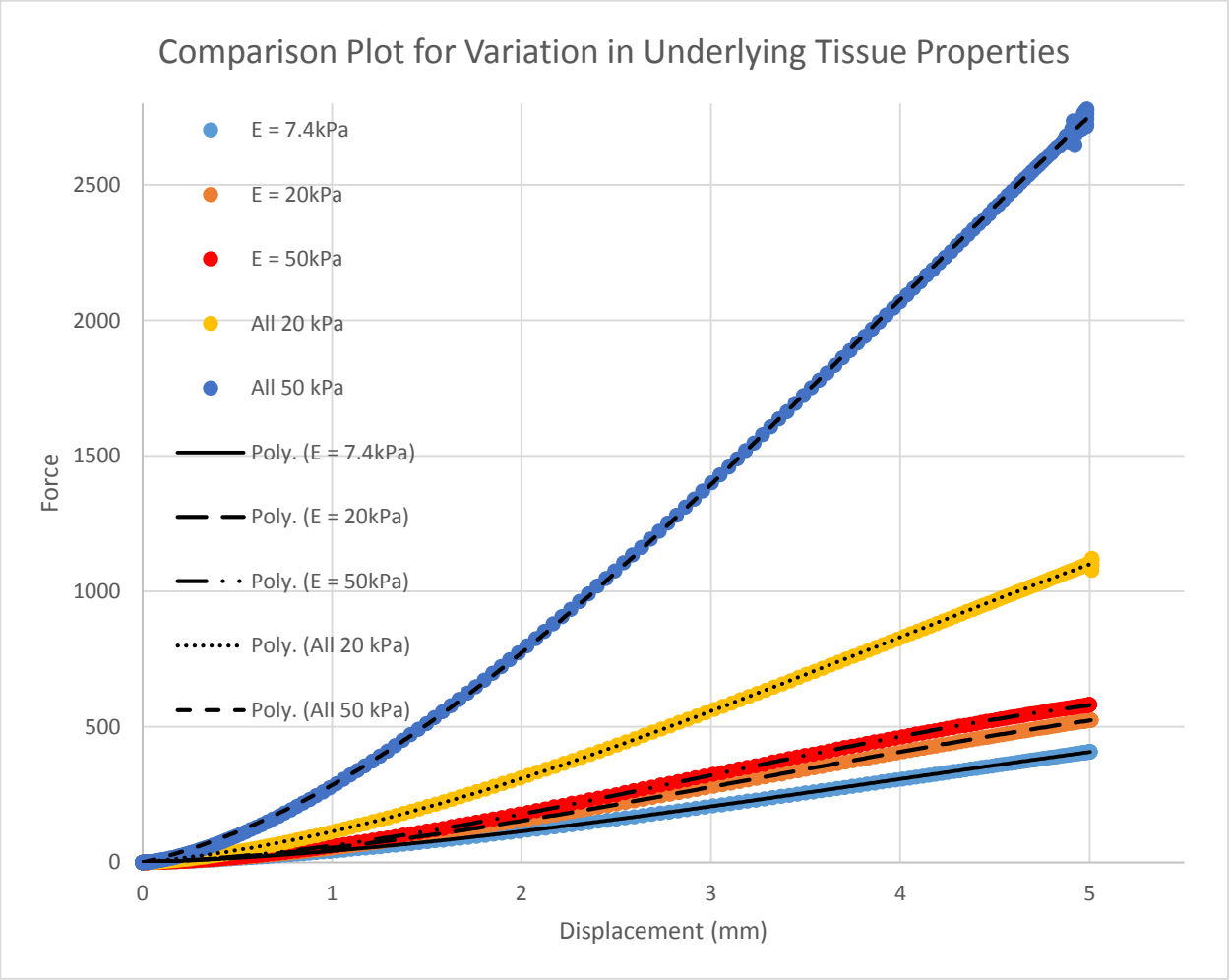

Figure 16: Comparison of all simulations for multiple tissue model.

When the defection contour plots were evaluated, the influence of the underlying tissue became even more evident (Figure 17). While the deflection propagated deep into the tissue with a constant 7.4 kPa elasticity, less influence of the defection was seen when the lower underlying tissue elasticity was increased to 20kPa. This confirms that the increased stiffness in the

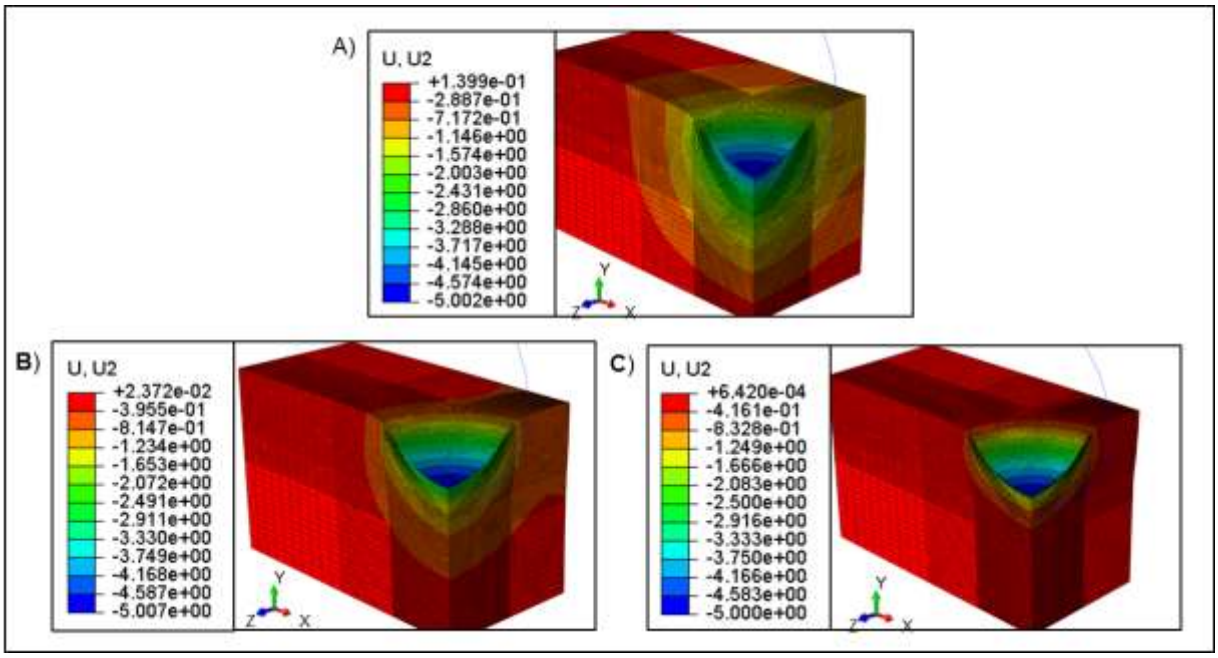

Figure 17: Contour plots showing the deflection throughout the tissue when the indenter was displaced 5 millimeters. (A) E value of 7.4kPa for entire tissue was used. (B) E values of 7.4kPa on upper tissue and 20kPa on underlying tissue were used. (C) E values of 7.4kPa on upper tissue and 50kPa on underlying tissue were used. Note scales are specific to each plot.

underlying tissue inhibits the influence of the deformation caused by the indenter. This trend continued with even less defection proliferating through the tissue with an underlying tissue elasticity of 50kPa.

The simulation allowed for further evaluation of stress. When the elastic modulus was a constant 7.4 kPa throughout the tissue, the stress was continuous across the boundary. The maximum stress of 6.11 kPa equated to a total stress on the full tissue of 24.44 kPa is located at the maximum deflection point (Figure 18A). An area of higher stress occurs towards the top of the deformation (Figure 19A). This is due to the stretching that occurs as the indenter is deforming

the tissue but the tissue does not completely conform to the indenter. By increasing the elastic modulus of the lower tissue to 20 kPa, the maximum stress is also increased to 8.46 kPa equating to 33.84kPa (Figure 18B). The stress magnitude is discontinuous across the boundary. The maximum stress is again located at the maximum displacement. The stress decreases as it moves away from the maximum deflection then begins to increase again towards the top and bottom surfaces of the upper tissue (Figure 19B). The increase towards the upper surface reflects the stress that is occurring due to the stretching separation between the indenter and the tissue as it is deflected. This value remains similar to the previous simulation value. The increase toward the bottom boundary reflects the stress due to the additional forces caused by the increase elastic modulus property in the lower tissue. This is exemplified again as the lower tissue elastic modulus is increased to 50 kPa. The maximum stress located at the maximum deflection is increased by to 9.93 kPa equating to 39.72 kPa (Figure 18C). The stress at the lower boundary is increased, however the upper boundary remains comparable to the previous two simulations (Figure 19C).

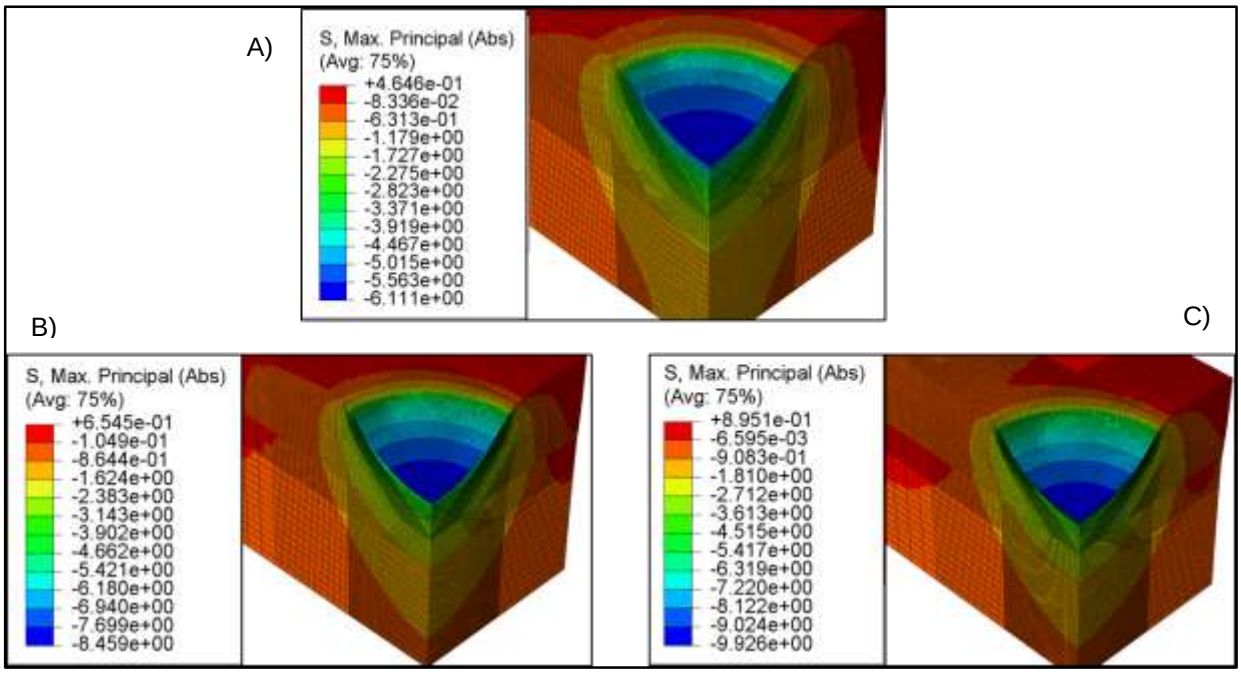

Figure 18: Maximum principle absolute stress for simulation with E value of 7.4 kPa for the upper 7mm and the lower 13mm tissue having an E value defined as (A) 7.4 kPa, (B) 20 kPa, and (C) 50 kPa. Note that the scales are unique to each contour plot.

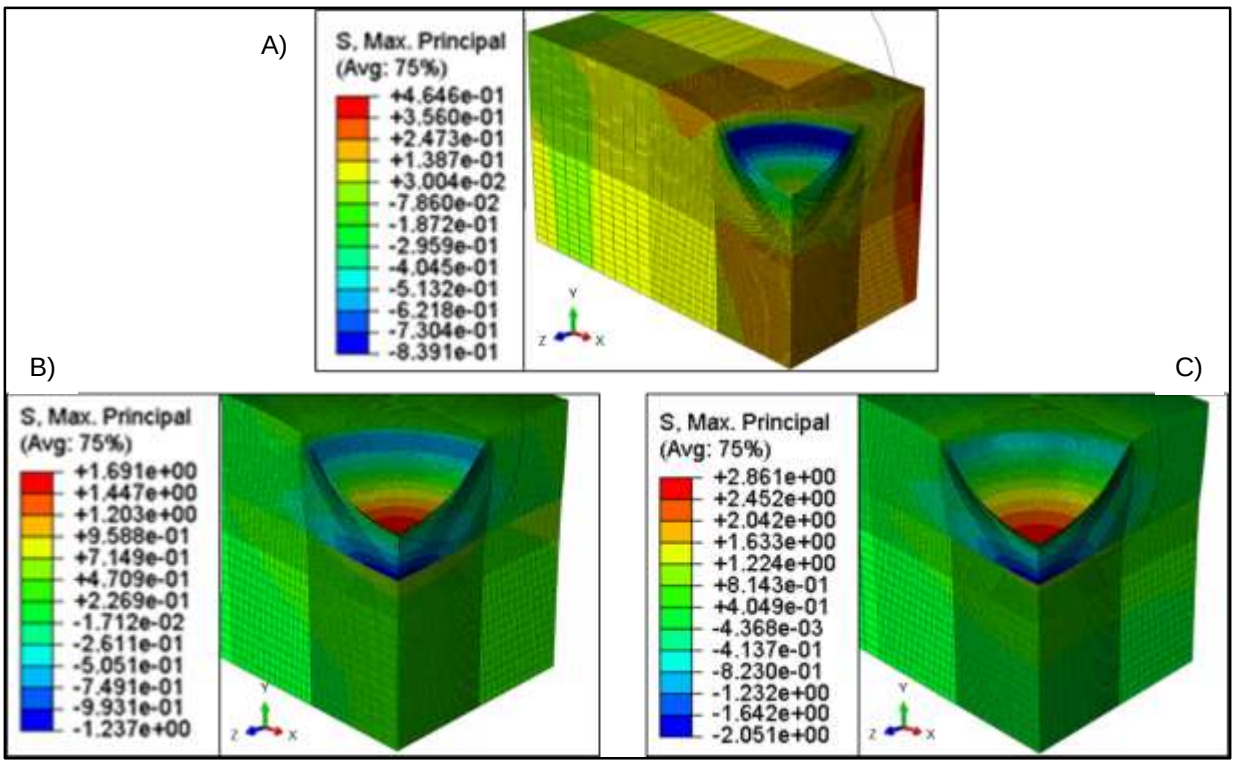

Figure 19: Maximum principle stress for simulation with E value of 7.4 kPa for the upper 7mm and the lower 13mm tissue having an E value defined as (A) 7.4 kPa, (B) 20 kPa, and (C) 50 kPa. Note that the scales are unique to each contour plot.

Additional stress and strain contour plots showing principal directions can be found in Appendix II – Stress and Strain Contour Plots.

Von Mises stress demonstrated similar responses to the deformation of the tissues with discontinuation seen in tissue with 2 different elastic modulus values (Figure 20). The maximum von Mises stresses are all located at the point of maximum deflection. While minimal in all cases, stress in the lower tissue are found through the depth of the tissue.

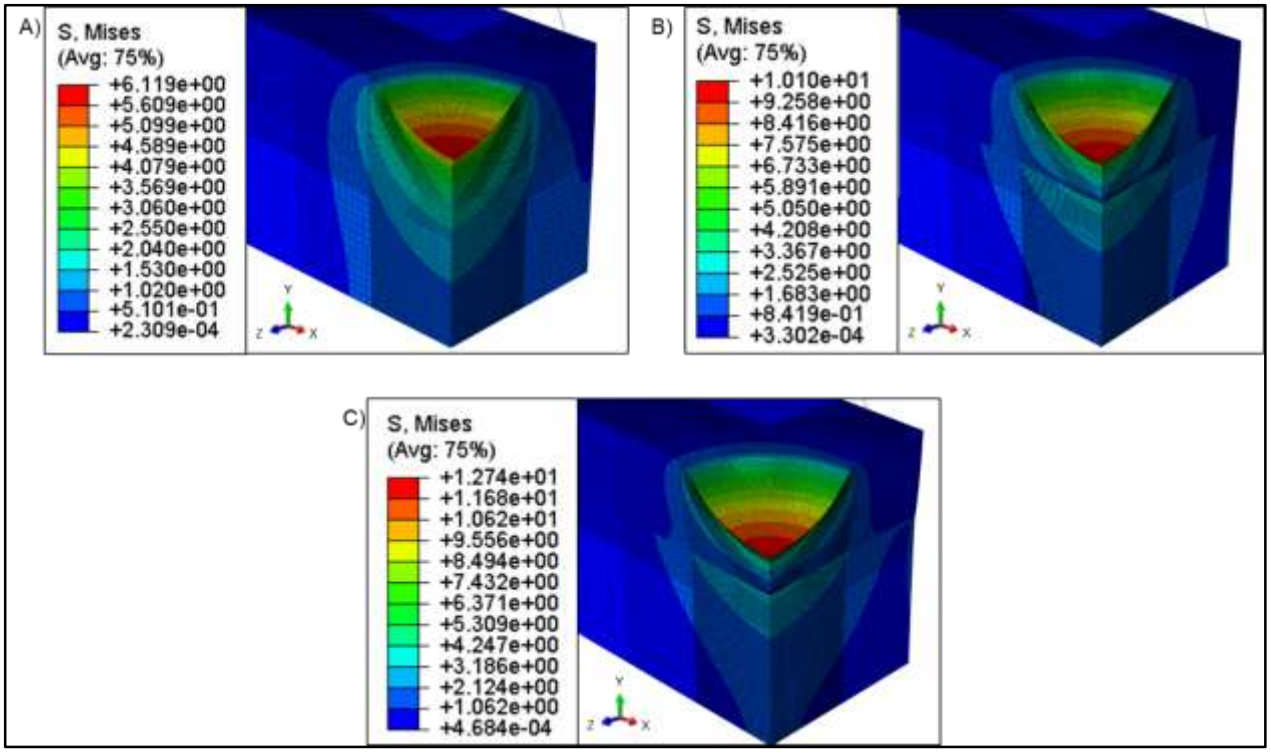

Figure 20: Von Mises stress contour plots for simulations containing upper tissue E value of 7.4 kPa and lower tissue E values at (A) 7.4 kPa, (B) 20 kPa, and (C) 50 kPa.

4. Conclusions and Future Work

4.1. Conclusions

A finite element model was developed for the purpose of simulating *in vivo*, human, vaginal tissue undergoing indentation testing with a spherical indenter. The model was created to supplement the Elevated-surface Vaginal Elastomer (EVE), and it was hypothesized that the model would provide a more thorough understanding of the tissue mechanics than EVE alone.

Results from a single tissue layer model were validated according to Hertz theory of elasticity. With five different mesh refinements, each showed congruency with the Hertz analytical solution for small deformation. This established the validity of the model for elastic deformation response. Simulated testing of large deformations exhibited stress and strain response deep within the tissue. These results lead to the exploration of a dual-layered tissue in order to understand the impacts of the tissue surrounding the vaginal tissue *in vivo*.

Because EVE measures the overall force, it was important to understand if measured values would be the result of vaginal tissue alone or if other surrounding tissue would impact the measured force needed to move the tissue a prescribed displacement. The vaginal tissue was defined to be 7 millimeters according to values obtained by Hsu [26]. The underlying tissue defined the remaining 13 millimeters of the model's 20 millimeter thick tissue. Varying the elasticity of the underlying tissue further demonstrated the impact to overall stiffness. The increase in force required to deform the tissue verified that the underlying tissue did influence the indentation test results. This provided insight to additional stiffness caused by surrounding organ tissues, skeletal muscles, or even bone that may be incorporated during *in vivo* testing. One example of this could be influences of bladder tissue. Since the bladder is located adjacent to the vaginal wall with connective tissue linking the two tissues, the stiffness of bladder tissue could cause changes in

forces felt during testing. Also, a full bladder versus an empty bladder could also causes variation in forces recorded by the EVE device. Inconsistencies in stiffness of adjoining tissue or contraction of muscles could lead to a broad range of elastic modulus values as has been seen in past published studies [15]. This is a significant result because it indicates that the instrument may be able to detect and evaluate elasticity of supporting tissue in diagnosing pelvic floor dysfunction.

The influence of the underlying tissue was reaffirmed by the stress patterns and discontinuities created in the contour plots. Higher stress values were found both at the maximum deformation site and at the interface of the two layers. When compared to stiffer materials, it was evident that the dominating factor was the elasticity of the upper vaginal tissue. When evaluating *in vivo* data, the degree of impact can be determined by the comparing the calculated stress values from the experimental data to the stress patterns of the FEA. This demonstrates how the FEA model will be useful for interpretation of *in vivo* data.

In addition to the underlying tissue, geometry of the tissue contributed to the force as well. This became evident when the single layer FEA results for an elasticity of 7.4 kPa were compared to preliminary EVE experimental results from tests performed on a phantom tissue with an estimated elasticity of 7.6 kPa. The cylindrical cavity in the cubic phantom tissue provided a snug fit for the EVE device when inserted. This lead to a displacement of 6 millimeter prior to the start of testing which caused a preloaded force on EVE. It was concluded that geometric differences contributed to these differences by the preload and also by strain due to the cylindrical shape. Since the force increased at a higher rate on the EVE data, this demonstrated the additional stresses that are felt within the cavity of the tissue. Using both results in conjunction creates limits for a range of properties in which the *in vivo* tissue results may fall. The extremities of a flat tissue and a small cylindrical shape can also be modified to reflect more congruency with each other.

Overall, the finite element analysis has provided a greater insight into the indentation tests by displaying the impacts within the tissue on force, stress, and strain. Additionally, influence of surrounding tissue was demonstrated. This increased understanding will be useful during the evaluation of *in vivo* data.

4.2. Future Work

This research project focused on providing a three-dimensional, finite element model to simulate elastic deformation of human vaginal tissue for the accompaniment of EVE *in vivo* testing. In order to verify congruency between the model and the device, experimental testing could be done on flat, phantom tissue with the same dimensions of those in the FE model. The test could then be performed at a true zero to 5 millimeter deflection. Conversely, a model could be created reflecting the dimensions of the phantom with a cylindrical cavity. However, creating a flat tissue would be a less intricate process. With the *in vivo* tissue expected to fall between these two extremes with possible large variability due to size, BMI, and parity, additional constraints could be applied to the current model with the intent mingling the tissue model with the experimental phantom tissue. Applying a symmetry constraint to a segment of the tissue top such that symmetry is applied in the Y direction, additional stresses and strains would emerge. This would be reflective of a continuous tissue on the edge of the tissue model versus a flat tissue. Changing the model in this way would still allow for a zero to five millimeter deflection.

Experimental *in vivo* outcomes may reflect hyperelastic properties of the tissue. Further investigation could focus on including hyperelastic properties into the FE model. This could be incorporated in two ways. A manual iteration could be conducted to match the force-displacement data between experimental data and FEA. This would be done by manually inputting elastic modulus values and running analyses until convergence is found to the experimental data. For a more automated process, the stress and strain would first need to be calculated from *in vivo*

experimentation data. Once the nominal stress and strain are known, these values can be inputted into the material properties of the tissue model and used to define the mechanical properties. The finite element analysis would then use these properties during simulated evaluation.

In order to reflect tissue fibers, anisotropic properties can be incorporated into the FE tissue. The 3-dimensional model was created for the purpose of adding anisotropy. By including this property, the stress and strains in the X and Z directions would either increase or decrease depending on the direction in which the fibers are modeled. This would in turn change the overall forces which may be observed in the data collected from experimentation.

5. References:

[1] Prevention USCfDCa. aids.gov. U.S. Department of Health and Human Services; 2014.

[2] Sokal DC, Karim QA, Sibeko S, Yende-Zuma N, Mansoor LE, Baxter C, et al. Safety of tenofovir gel, a vaginal microbicide, in South African women: results of the CAPRISA 004 Trial. Antiviral therapy. 2013;18:301-10.

[3] van der Straten A, Mayo A, Brown ER, Amico KR, Cheng H, Laborde N, et al. Perceptions and Experiences with the VOICE Adherence Strengthening Program (VASP) in the MTN-003 Trial. AIDS and behavior. 2015;19:770-83.

[4] Martins P, Pena E, Calvo B, Doblare M, Mascarenhas T, Natal Jorge R, et al. Prediction of nonlinear elastic behaviour of vaginal tissue: experimental results and model formulation. Computer methods in biomechanics and biomedical engineering. 2010;13:327-37.

[5] Britannica EoE. Vagina. Encyclopedia Britannica. Encyclopedia Britannica Online2014.

[6] Ahn B, Kim J. Measurement and characterization of soft tissue behavior with surface deformation and force response under large deformations. Medical image analysis. 2010;14:138-48.

[7] Oyen ML. Analytical Techniques for Indentaton of Viscoelastic Materials. Philosophical Magazine. 2006:5625-41.

[8] Mencik J, He LH, Swain MV. Determination of viscoelastic-plastic material parameters of biomaterials by instrumented indentation. Journal of the mechanical behavior of biomedical materials. 2009;2:318-25.

[9] Rubod C, Boukerrou M, Brieu M, Dubois P, Cosson M. Biomechanical properties of vaginal tissue. Part 1: new experimental protocol. The Journal of urology. 2007;178:320-5; discussion 5.

[10] Samur E, Sedef M, Basdogan C, Avtan L, Duzgun O. A robotic indenter for minimally invasive measurement and characterization of soft tissue response. Medical image analysis. 2007;11:361-73.

[11] Lin DC, Shreiber DI, Dimitriadis EK, Horkay F. Spherical indentation of soft matter beyond the Hertzian regime: numerical and experimental validation of hyperelastic models. Biomechanics and modeling in mechanobiology. 2009;8:345-58.

[12] Carson WC, Gerling GJ, Krupski TL, Kowalik CG, Harper JC, Moskaluk CA. Material characterization of ex vivo prostate tissue via spherical indentation in the clinic. Medical engineering & physics. 2011;33:302-9.

[13] Rubod C, Boukerrou M, Brieu M, Jean-Charles C, Dubois P, Cosson M. Biomechanical properties of vaginal tissue: preliminary results. International urogynecology journal and pelvic floor dysfunction. 2008;19:811-6.

[14] Epstein L. Systemic and Vaginal Biomechanical Properties of Women with Normal Vaginal Support and Pelvic Organ Prolapse. American Journal of Obstetrics & Gynocology. 2007;197:1-6.

[15] Egorov V, van Raalte H, Lucente V. Quantifying vaginal tissue elasticity under normal and prolapse conditions by tactile imaging. International urogynecology journal. 2012;23:459-66.

[16] Chuong CJ, Ma M, Eberhart RC, Zimmern P. Viscoelastic properties measurement of the prolapsed anterior vaginal wall: a patient-directed methodology. European journal of obstetrics, gynecology, and reproductive biology. 2014;173:106-12.

[17] Choi AP, Zheng YP. Estimation of Young's modulus and Poisson's ratio of soft tissue from indentation using two different-sized indentors: finite element analysis of the finite deformation effect. Medical & biological engineering & computing. 2005;43:258-64.

[18] Jin H, Lewis JL. Determination of Poisson's ratio of articular cartilage by indentation using different-sized indenters. Journal of biomechanical engineering. 2004;126:138-45.

[19] Liu Y. A Nonlinear Finite Element Model of Soft Tissue Indentation. Medical Simulation; International Symposium. 2004:67-76.

[20] Hu T, Desai JP. Soft-tissue material properties under large deformation: strain rate effect. Conference proceedings : Annual International Conference of the IEEE Engineering in Medicine and Biology Society IEEE Engineering in Medicine and Biology Society Annual Conference. 2004;4:2758-61.

[21] McKee CT, Last JA, Russell P, Murphy CJ. Indentation versus tensile measurements of Young's modulus for soft biological tissues. Tissue engineering Part B, Reviews. 2011;17:155-64.

[22] Mureithi MW, Poole D, Naranbhai V, Reddy S, Mkhwanazi NP, Sibeko S, et al. Preservation HIV-1-specific IFNgamma+ CD4+ T-cell responses in breakthrough infections after exposure to tenofovir gel in the CAPRISA 004 microbicide trial. Journal of acquired immune deficiency syndromes. 2012;60:124-7.

[23] Barnhart KT, Izquierdo A, Pretorius ES, Shera DM, Shabbout M, Shaunik A. Baseline dimensions of the human vagina. Human reproduction. 2006;21:1618-22.

[24] Ward SR, Lieber RL. Density and hydration of fresh and fixed human skeletal muscle. Journal of biomechanics. 2005;38:2317-20.

[25] Johnson KL. Contact Mechanics: Cambridge University Press; 1985.

[26] Hsu Y, Chen L, Delancey JO, Ashton-Miller JA. Vaginal thickness, cross-sectional area, and perimeter in women with and those without prolapse. Obstetrics and gynecology. 2005;105:1012-7.

6. Appendix I – Hertz Theory of Elasticity

Hertz theory of elasticity was utilized for validation of the FE model. Equations were taken from *Contact Mechanics* by Johnson [25]. Maple software was used to complete the calculations below.

Assumptions:

1) a<<R
2) Tissue modeled as an elastic half-space.
3) Surfaces are continuous
4) Interaction is frictionless and nonconforming

$R := 9.65 = 9.65\ mm$ - Indenter radius

$a := 0.096 = 0.096\ mm$ - contact radius

$E1 := 7.4 = 7.4\ \frac{kg}{mm \cdot s^2}$ - Young's Modulus of the tissue

$\nu 1 := 0.48 = 0.48$ - Poisson's Ratio of the tissue

$\delta = \frac{a^2}{R} = \delta = 0.0009550259067\ mm$ - Displacement of the indenter into the tissue

$E := \left(\frac{\left(1 - \nu 1^2\right)}{E1} \right)^{-1} = 9.615384613\ \frac{kg}{mm \cdot s^2}$ -

Note that the original equation of $\frac{1}{E^*} = \frac{1-\nu_1^2}{E_1} + \frac{1-\nu_2^2}{E_2}$ includes E_2 and ν_2, but due to the rigidity of the indenter, the second term is negligible.

For force F:

$F := \frac{4}{3} \cdot \frac{a^3 \cdot E}{R} = 0.001175416500\ \frac{kg \cdot mm}{s^s}$

For contact pressure p:

$$p := \frac{3 \cdot F}{2 \cdot 3.14 \cdot a^2} = 0.06092715903 \ \frac{kg}{mm \cdot s^2}$$

For stress σ:

$$\sigma := \frac{1}{3} \cdot (1 - 2 \cdot \nu l) \cdot p = 0.0008123621203 \ \frac{kg}{mm \cdot s^2}$$

7. Appendix II – Stress and Strain Contour Plots

Additional stress and strain contour plots have been provided to show clarity in directional influence. Figure 21, Figure 22, and Figure 23 show strain contour plots for multilayered tissue. Elasticity of top tissue is 7.4kPa. Bottom tissue elasticity specified in caption. Comparing the max principal strain shows the strain value become more positive as the bottom tissue increases in stiffness. Evaluating the strains in the principal directions shows that positive strain in the X and Z directions becomes greater than the negative strain in the Y direction. This difference is then reflected in the max principal strain plot.

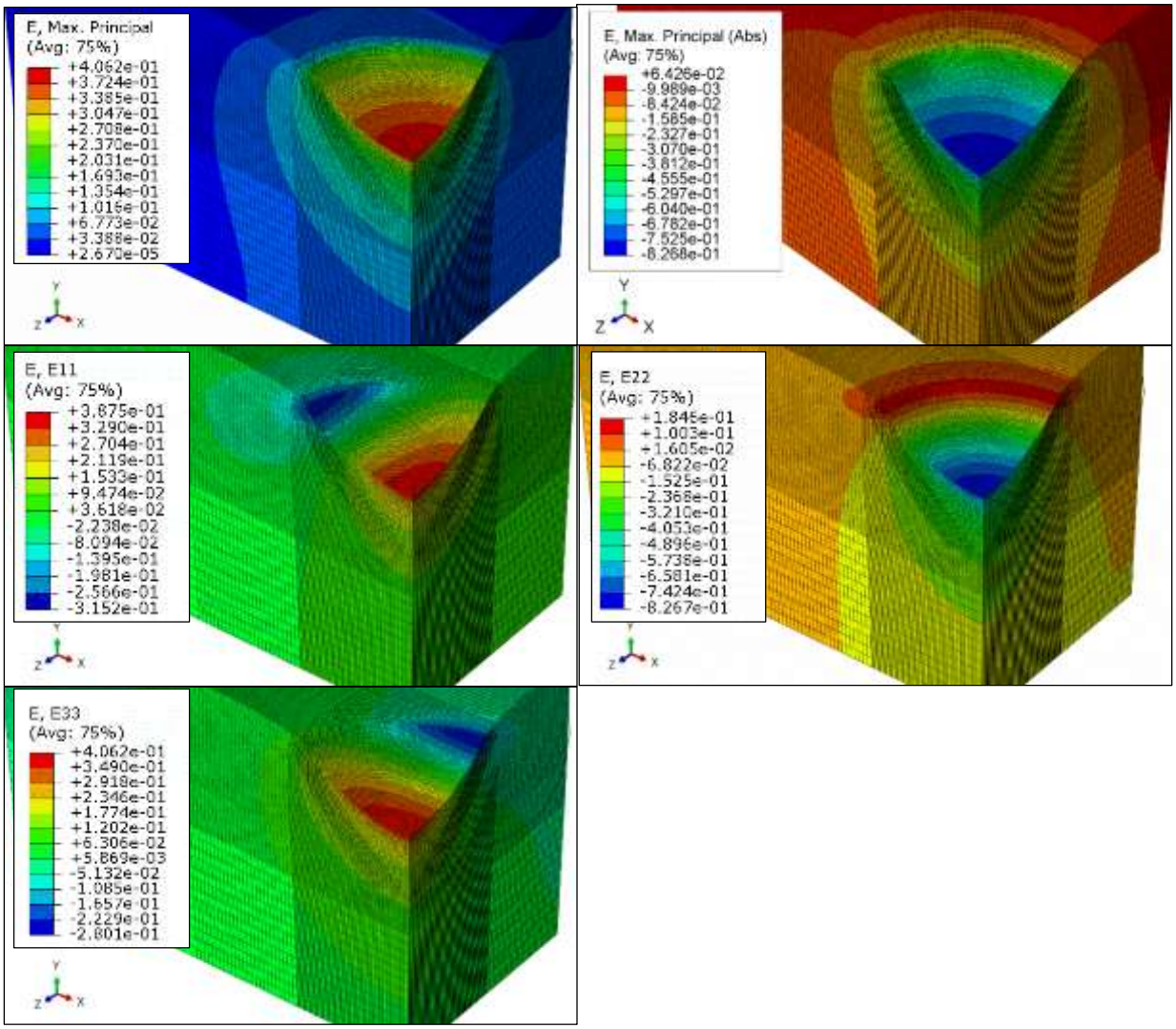

Figure 21 Strain contour plots comparing the directional strain tensor components in order to identify directional influence. Plots show strain for tissue elasticity of 7.4kPa.

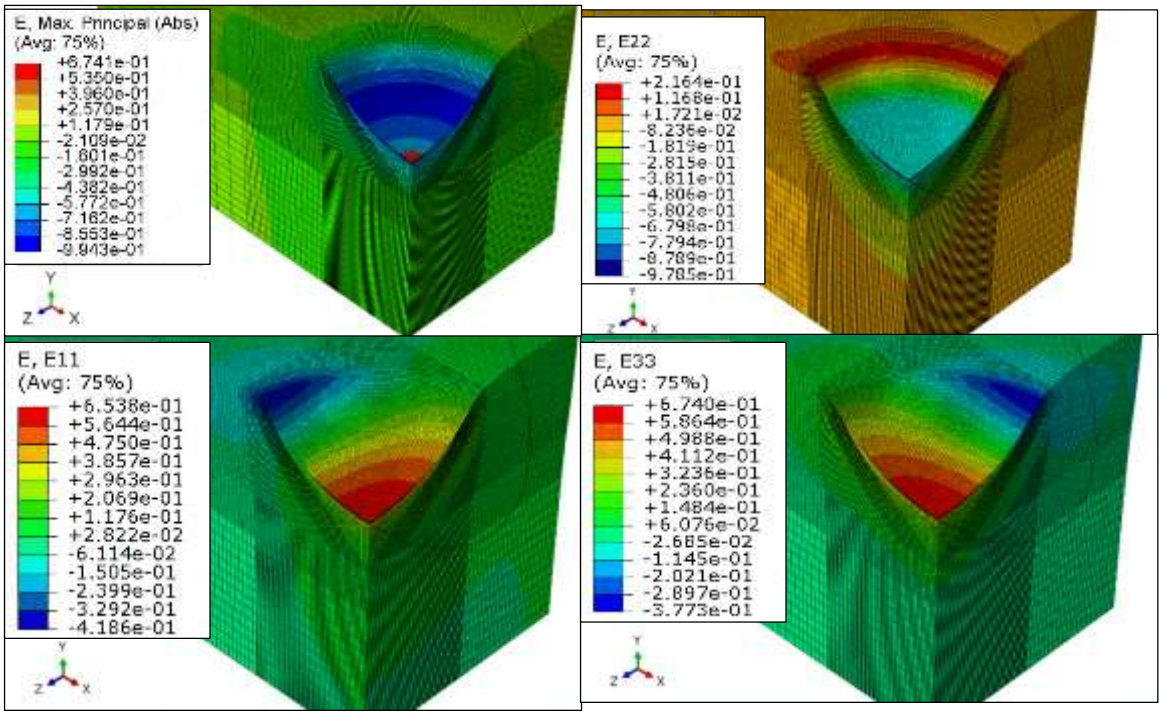

Figure 22: Strain contour plots showing directional tensors to show influence for max strain. Elasticity for contours is 20kPa.

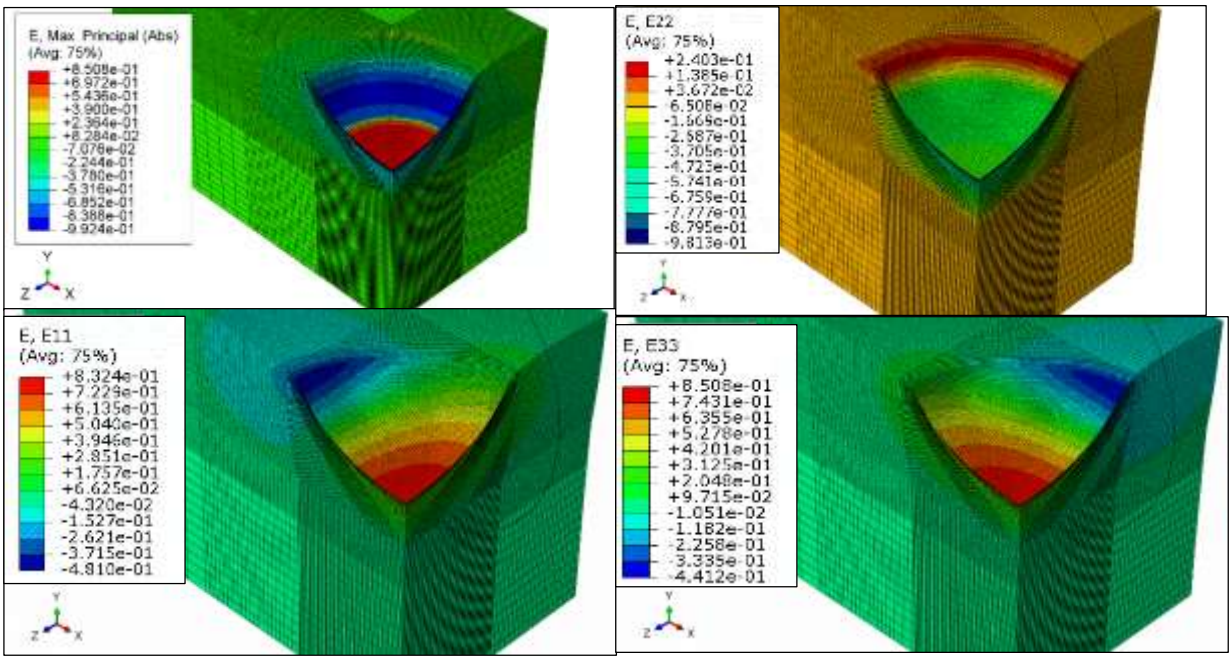

Figure 23: Strain contour plots showing directional tensors to show influence for max strain. Elasticity for contours is 50kPa.

Stress contour plots comparing max principal stress with tensor directional stresses to understand directional influence. Tissue is multilayered with top tissue elasticity at 7.4kPa and bottom tissue as specified in the caption.

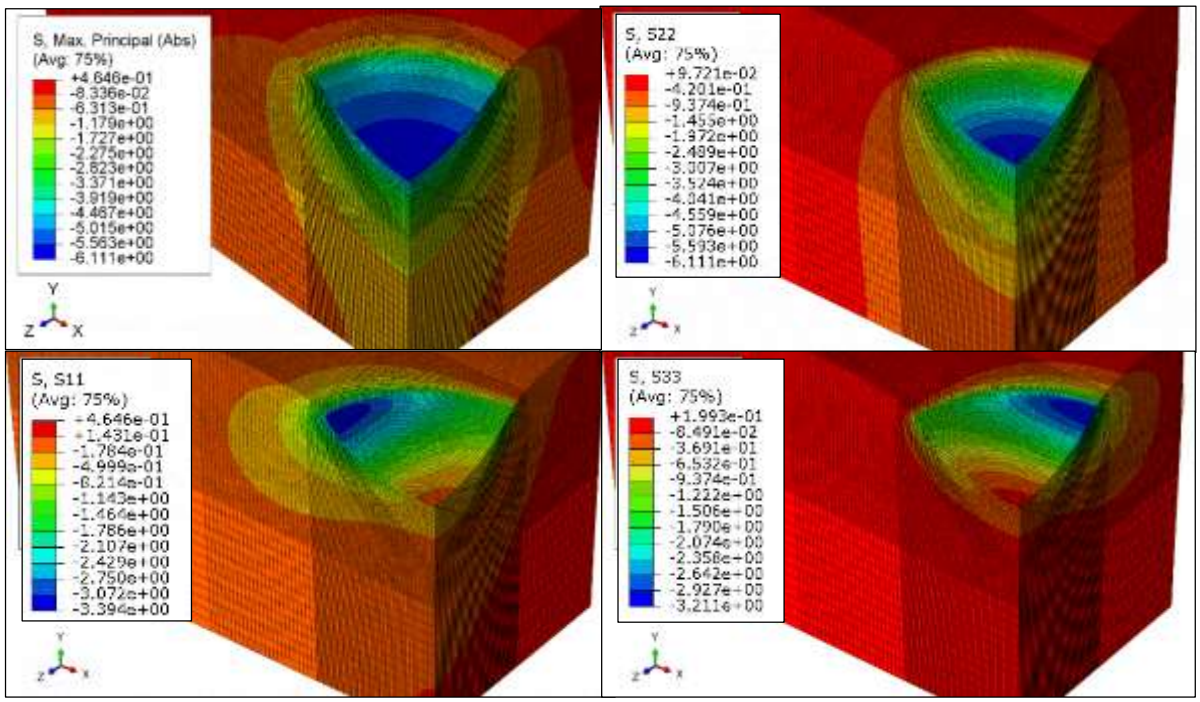

Figure 24: Stress contour plot comparison. Bottom tissue elasticity equal to 7.4 kPa.

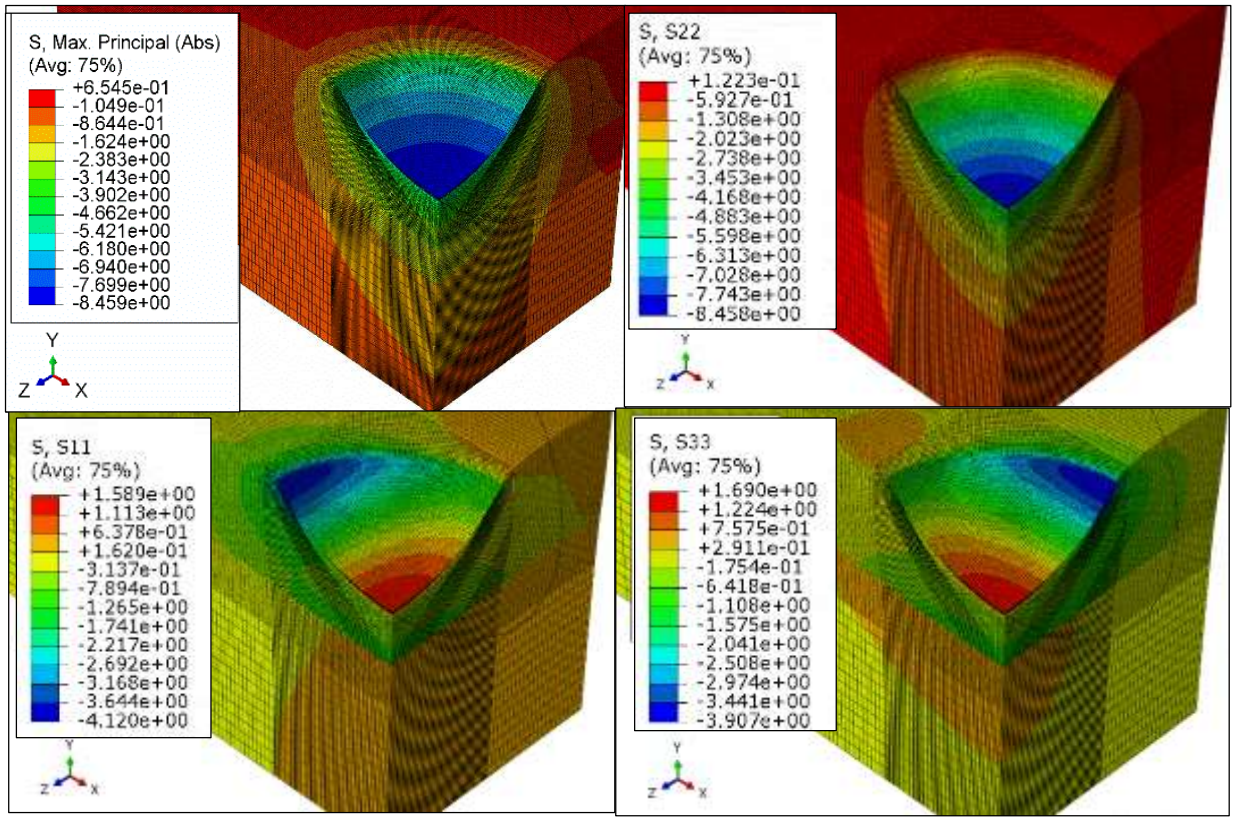

Figure 25: Stress contour plot comparison. Bottom tissue elasticity equal to 20kPa.

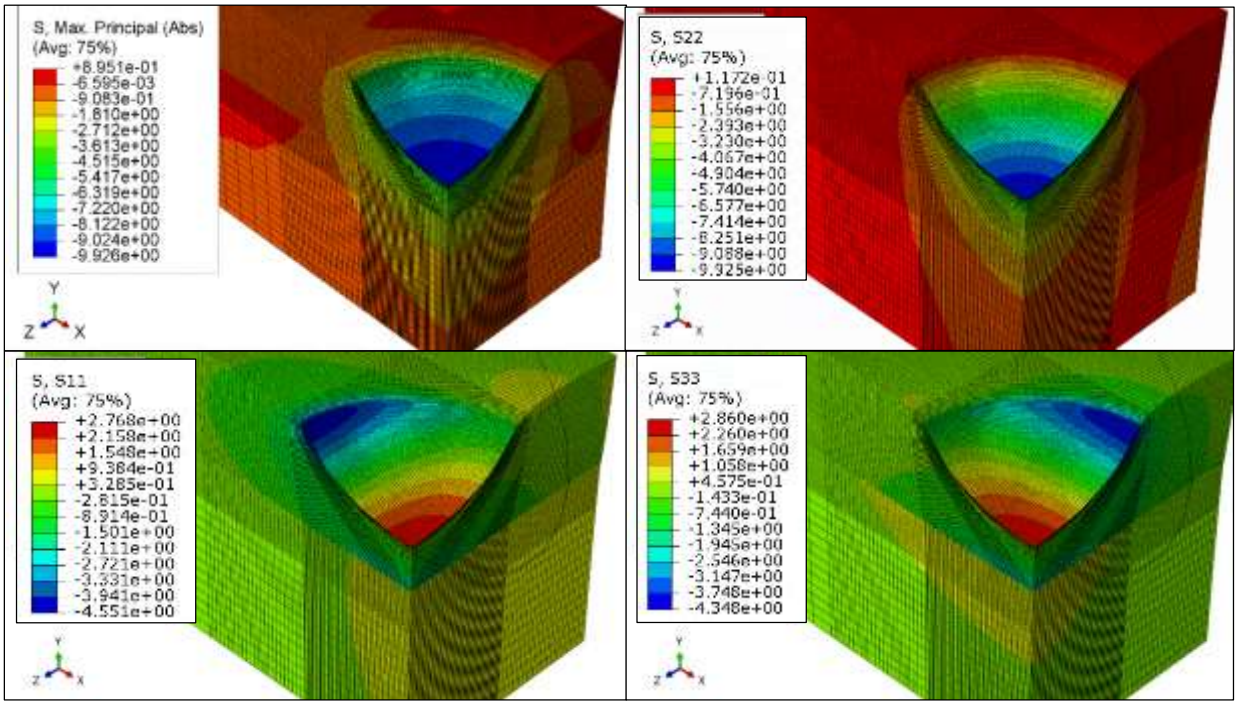

Figure 26: Stress contour plot comparison. Bottom tissue equal to 50kPa.